Appl. Math. Mech. -Engl. Ed., **41**(2), 233–260 (2020)

Applied Mathematics and Mechanics (English Edition)

https://doi.org/10.1007/s10483-020-2564-5

Nonlinear primary resonance analysis of nanoshells including vibrational mode interactions based on the surface elasticity theory*

A. SARAFRAZ[1], S. SAHMANI[2,†], M. M. AGHDAM[1]

1. Mechanical Engineering Department, Amirkabir University of Technology, Tehran 15875-4413, Iran;
2. School of Science and Technology, The University of Georgia, Tbilisi 0171, Georgia

(Received Aug. 10, 2019 / Revised Sept. 25, 2019)

Abstract The deviation from the classical elastic characteristics induced by the free surface energy can be considerable for nanostructures due to the high surface to volume ratio. Consequently, this type of size dependency should be accounted for in the mechanical behaviors of nanoscale structures. In the current investigation, the influence of free surface energy on the nonlinear primary resonance of silicon nanoshells under soft harmonic external excitation is studied. In order to obtain more accurate results, the interaction between the first, third, and fifth symmetric vibration modes with the main oscillation mode is taken into consideration. Through the implementation of the Gurtin-Murdoch theory of elasticity into the classical shell theory, a size-dependent shell model is developed incorporating the effect of surface free energy. With the aid of the variational approach, the governing differential equations of motion including both of the cubic and quadratic nonlinearities are derived. Thereafter, the multi-time-scale method is used to achieve an analytical solution for the nonlinear size-dependent problem. The frequency-response and amplitude-response of the soft harmonic excited nanoshells are presented corresponding to different values of shell thickness and surface elastic constants as well as various vibration mode interactions. It is depicted that through consideration of the interaction between the higher symmetric vibration modes and the main oscillation mode, the hardening response of nanoshell changes to the softening one. This pattern is observed corresponding to both of the positive and negative values of the surface elastic constants and the surface residual stress.

Key words nanostructure, nonlinear dynamics, surface stress, mode interaction, multi-time-scale method

Chinese Library Classification O322
2010 Mathematics Subject Classification 74H55

* Citation: SARAFRAZ, A., SAHMANI, S., and AGHDAM, M. M. Nonlinear primary resonance analysis of nanoshells including vibrational mode interactions based on the surface elasticity theory. *Applied Mathematics and Mechanics* (*English Edition*), **41**(2), 233–260 (2020) https://doi.org/10.1007/s10483-020-2564-5

† Corresponding author, E-mail: sahmani@aut.ac.ir

1 Introduction

In the last decade, in order to design structures with outstanding mechanical and electrical characteristics including optical properties, nanostructures have been manufactured via a few molecular manipulations. These miniaturized small-scaled structures have been considered as basic elements for several applications, such as nanosensors, transistors, and micro-truss structures. Consequently, it is fundamentally significant to predict the size-dependent mechanical behaviors of nanostructures. Because atomistic simulations are often very time-consuming, and controlled nanoscaled experiments are so hard to implement, continuum mechanics has been more attractive for researchers to analyze mechanical responses of nanostructures. For this purpose, various non-classical continuum theories of elasticity have been introduced and applied to capture different size dependencies in mechanical behaviors of small-scaled structures.

Togun and Bagdatli[1] performed a nonlinear vibration analysis of tensioned nanobeams with different end supported on the basis of the modified couple stress theory of elasticity. Bornassi and Haddadpour[2] investigated the nonlocal dynamical pull-in instability of an electrostatic actuated carbon nanotube-based nanodevices. Guo et al.[3] constructed a modified couple stress plate model for three-dimensional free vibration of anisotropic layered nanoplates. Li et al.[4] examined the nonlocal resonance of an axially moving viscoelastic piezoelectric nanoplate under thermo-electro-mechanical forces. Zhang et al.[5] implemented the nonlocal elasticity theory into the classical plate theory to model the nonlinear vibrations of graphene sheets using the meshfree technique. Lu et al.[6] proposed a nonlocal strain gradient shear deformable beam model for size-dependent free vibrations of nanobeams. Liu et al.[7] put the nonlocal elasticity and the Kelvin model to capture the size effect on the vibration and buckling characteristics of the double-viscoelastic-functionally graded nanoplate system. Zhang et al.[8] presented analytical solutions for buckling and vibration behaviors of lattice-based nonlocal continualized circular arches at the nanoscale. Yang and He[9] constructed a microstructure-dependent model for vibration and buckling responses of orthotropic functionally graded microplates. Fang et al.[10] developed a size-dependent three-dimensional dynamic model on the basis of the modified couple stress elasticity theory for the rotating functionally graded Euler-Bernoulli microbeam. Apuzzo et al.[11] employed the modified nonlocal strain gradient theory of elasticity to analyze size dependency in axial and flexural free vibrations of Euler-Bernoulli nanoscaled beams. Kiani and Pakdaman[12] explored the free transverse thermos-elastic vibrations of monolayers from double-walled carbon nanotubes under heat dissipation. Wang et al.[13] studied the free transverse vibrations of axially moving nanobeams including nonlocality and strain gradient size dependencies. Thanh et al.[14] utilized the isogeometric technique for size-dependent analysis of functionally graded nanocomposite nanoplates modeled via the higher-order shear deformation theory together with the modified couple stress theory. Sahmani et al.[15–17] took the nonlocality and strain gradient size effect into the nonlinear bending and vibrations of multilayer functionally graded micro/nanostructures reinforced with graphene platelets. Wang[18] proposed a novel differential quadrature element method for free vibration analysis of hybrid Euler-Bernoulli beams based on the nonlocal theory of elasticity. Shen et al.[19] analyzed the transverse dynamics of microtubules under axial load and variable transverse load on the basis of the nonlocal strain gradient theory of elasticity. Tang et al.[20] studied the nonlocal strain gradient vibration response of small-scaled beams including Poisson's ratio and thickness effects. Jalaei et al.[21] predicted the dynamic instability of functionally graded Timoshenko nanobeams subject to thermal and magnetic fields based upon the nonlocal strain gradient elasticity theory. Sahmani and Safaei[22–23] employed the nonlocal strain gradient theory of elasticity for nonlinear free and forced vibration characteristics of bi-directional functionally graded micro/nanobeams. Jalaei and Civalek[24] anticipated the size-dependent dynamic instability of embedded graphene sheet incorporating thermal effects. Zhang et al.[25] developed multi-scale modeling for Euler-Bernoulli nanobeams with a large deflection on the basis of the

nonlocal strain gradient elasticity. Sahmani et al.[26] explored nonlinear mechanical characteristics of micro/nanostructures in the presence of various types of size dependency. Wang et al.[27] investigated the nonlinear free vibration response of piezoelectric cylindrical nanoshells resting on a viscoelastic foundation.

Reduction in the dimension of a structure results in a higher surface to volume ratio. Consequently, there is a difference between material properties associated with free surfaces of an elastic medium and those of the bulk. This issue is attributed to the fact that the necessary conditions for equilibration of free surface atoms are different from those required for bulk atoms. In other words, there is excessive energy within the free surface layers namely as the surface free energy which causes to make a change in mechanical behaviors of micro/nanostructures. In order to capture this type of size dependency, Gurtin and Murdoch[28–29] introduced a generic theoretical model within the framework of the continuum elasticity. Several investigations have been carried out in recent years using the Gurtin-Murdoch elasticity theory to analyze mechanical behaviors of micro/nanostructures. Wang and Feng[30] developed a theoretical model directed towards a study on the effects of surface elasticity and surface residual stress on the natural frequency of microbeams. Luo and Xiao[31] explored the interaction between a screw dislocation and nano inhomogeneity including interface stress effects using the Gurtin-Murdoch continuum model. Zhao and Rajapakse[32] incorporated the surface free energy effects on the elastic field within an isotropic elastic layer under surface loading. Wang et al.[33] employed the Gurtin-Murdoch theory of elasticity to analyze the influences of the residual surface stress and surface tension on the elastic properties of nanostructures. Chiu and Chen[34] presented a closed-form analytical solution for bending and resonance characteristics of nanowires with various end supports. Shaat et al.[35] combined the Gurtin-Murdoch elasticity with the modified couple stress continuum theory to investigate the size-dependent bending behavior of nanoplates. Sahmani et al.[36] examined the nonlinear forced vibrations of third-order shear deformable nanobeams in the presence of surface stress effects. Also, Sahmani and Aghdam[37] captured the surface free energy effects on the nonlinear instability of cylindrical nanoshells under axial compression. Lu et al.[38] investigated the coupling effects of nonlocal stress and surface stress on the size-dependent mechanical responses of Kirchhoff and Mindlin nanoplates. Sun et al.[39] studied the buckling behavior of piezoelectric nanoshells in the presence of nonlocality and surface stress effects. Lu et al.[40] presented a unified size-dependent plate model for buckling analysis of nanoplates including nonlocal strain gradient size dependency and surface stress effects. Sarafraz et al.[41] analyzed the nonlinear secondary resonance of nanobeams under subharmonic and superharmonic excitations based on the surface elasticity theory.

The prime aim of this work is to capture the surface free energy effects on the nonlinear primary resonance of soft harmonic excited nanoshell incorporating the vibration mode interaction. For this purpose, the non-classical governing differential equations of motion are derived based upon the Gurtin-Murdoch theory of elasticity. Thereafter, with the aid of the multi-time-scale solution methodology, the size-dependent frequency-response and amplitude-response are achieved corresponding to various values of surface elastic constants, surface residual stress, and different interactions between the main vibration mode and the first, third, and fifth symmetric modes.

2 Derivation of the equations of motion

As illustrated in Fig. 1, a cylindrical nanoshell with free surface layers is considered. In accordance with the attached coordinate system and the classical shell theory, the components of the displacement vector can be expressed as

$$\begin{cases} u_1(x,\theta,z,t) = u(x,\theta,t) - z\dfrac{\partial w(x,\theta,t)}{\partial x}, \\ u_2(x,\theta,z,t) = v(x,\theta,t) - \dfrac{z}{R}\dfrac{\partial w(x,\theta,t)}{\partial \theta}, \quad u_3(x,\theta,z,t) = w(x,\theta,t), \end{cases} \tag{1}$$

where u, v, and w are the displacements of the midplane along x-axis, θ-axis, and z-axis, respectively. Also, R and t represent the radius of the nanoshell and time, respectively.

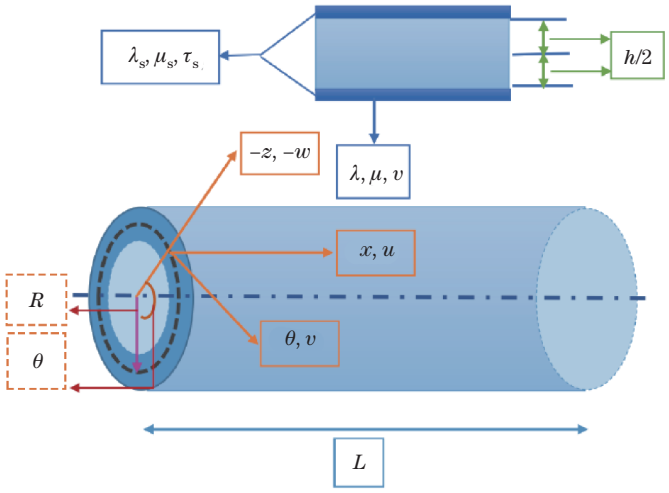

Fig. 1 Schematic representation of a silicon nanoshell with free surface layers and the attached coordinate system

On the basis of the Dannell's shell theory and von Karman geometric nonlinearity, the strain-displacement relationships can be given as

$$\begin{cases} \varepsilon_{xx} = \varepsilon^0_{xx} + z\kappa_x, \\ \varepsilon_{\theta\theta} = \varepsilon^0_{\theta\theta} + z\kappa_{\theta\theta}, \\ \gamma_{x\theta} = \gamma^0_{x\theta} + z\kappa_{x\theta}, \end{cases} \tag{2}$$

where

$$\begin{cases} \varepsilon^0_{xx} = \dfrac{\partial u}{\partial x} + \dfrac{1}{2}\left(\dfrac{\partial w}{\partial x}\right)^2, \quad \varepsilon^0_{\theta\theta} = \dfrac{1}{R}\dfrac{\partial v}{\partial \theta} - \dfrac{w}{R} + \dfrac{1}{2}\left(\dfrac{1}{R}\dfrac{\partial w}{\partial \theta}\right)^2, \\ \gamma^0_{x\theta} = \dfrac{1}{R}\dfrac{\partial u}{\partial \theta} + \dfrac{\partial v}{\partial x} + \dfrac{1}{R}\dfrac{\partial w}{\partial x}\dfrac{\partial w}{\partial \theta}, \\ \kappa_{xx} = -\dfrac{\partial^2 w}{\partial x^2}, \quad \kappa_{\theta\theta} = -\dfrac{1}{R^2}\dfrac{\partial^2 w}{\partial \theta^2}, \quad \kappa_{x\theta} = -\dfrac{2}{R}\dfrac{\partial^2 w}{\partial x \partial \theta}. \end{cases} \tag{3}$$

Within the framework of the linear theory of elasticity, the constitutive stress-strain relationship takes the following form:

$$\begin{pmatrix} \sigma_{xx} \\ \sigma_{\theta\theta} \\ \sigma_{x\theta} \end{pmatrix} = \begin{pmatrix} \lambda + 2\mu & \lambda & 0 \\ \lambda & \lambda + 2\mu & 0 \\ 0 & 0 & \mu \end{pmatrix} \begin{pmatrix} \varepsilon_{xx} \\ \varepsilon_{\theta\theta} \\ \gamma_{x\theta} \end{pmatrix}, \tag{4}$$

where the Lame's constants can be introduced in terms of Young's modulus and Poisson's ratio as below,

$$\lambda = \frac{\nu E}{1-\nu^2}, \quad \mu = \frac{E}{2(1+\nu)}. \tag{5}$$

In addition, based upon the Gurtin-Murdoch theory of elasticity, the surface stress components can be defined as functions of strain components, surface Lame's constants $(\lambda_{\rm s}, \mu_{\rm s})$, and surface residual stress $(\tau_{\rm s})$ as follows[28–29]:

$$\begin{cases} \sigma^{\rm s}_{\alpha\beta} = \tau_{\rm s}\delta_{\alpha\beta} + (\tau_{\rm s} + \lambda_{\rm s})\varepsilon_{\gamma\gamma}\delta_{\alpha\beta} + 2(\mu_{\rm s} - \tau_{\rm s})\varepsilon_{\alpha\beta} + \tau_{\rm s}u^{\rm s}_{\alpha,\beta}, \\ \sigma^{\rm s}_{\alpha z} = \tau_{\rm s}u^{\rm s}_{z,\alpha}. \end{cases} \tag{6}$$

As a consequence, one will have

$$\begin{cases} \sigma^{\rm s}_{xx} = (\lambda_{\rm s} + 2\mu_{\rm s})\varepsilon_{xx} + (\tau_{\rm s} + \lambda_{\rm s})\varepsilon_{\theta\theta} + \tau_{\rm s} - \dfrac{\tau_{\rm s}}{2}\Big(\dfrac{\partial w}{\partial x}\Big)^2, \\ \sigma^{\rm s}_{\theta\theta} = (\lambda_{\rm s} + 2\mu_{\rm s})\varepsilon_{\theta\theta} + (\tau_{\rm s} + \lambda_{\rm s})\varepsilon_{xx} + \tau_{\rm s} + \dfrac{\tau_{\rm s}}{R} - \dfrac{\tau_{\rm s}}{2}\Big(\dfrac{1}{R}\dfrac{\partial w}{\partial\theta}\Big)^2, \\ \sigma^{\rm s}_{x\theta} = \mu_{\rm s}\gamma_{x\theta} - \tau_{\rm s}\Big(\dfrac{\partial v}{\partial x} + \dfrac{1}{R}\dfrac{\partial w}{\partial x}\dfrac{\partial w}{\partial\theta} + \dfrac{z}{R}\dfrac{\partial^2 w}{\partial x\partial\theta}\Big), \\ \sigma^{\rm s}_{\theta x} = \mu_{\rm s}\gamma_{x\theta} - \tau_{\rm s}\Big(\dfrac{1}{R}\dfrac{\partial u}{\partial\theta} + \dfrac{1}{R}\dfrac{\partial w}{\partial x}\dfrac{\partial w}{\partial\theta} + \dfrac{z}{R}\dfrac{\partial^2 w}{\partial x\partial\theta}\Big), \\ \sigma^{\rm s}_{xz} = \tau_{\rm s}\dfrac{\partial w}{\partial x}, \\ \sigma^{\rm s}_{xz} = \dfrac{\tau_{\rm s}}{R}\dfrac{\partial w}{\partial\theta}. \end{cases} \tag{7}$$

Generally, in the classical continuum models, the stress component of σ_{zz} is ignored, since its value is very small in comparison with other stress components. However, in a continuum model based on the surface theory of elasticity, in order to satisfy the equilibrium necessities, it is required to be taken into account. For this purpose, it is assumed that

$$\sigma_{zz} = \frac{\dfrac{\partial\sigma^{S^+}_{xz}}{\partial x} + \dfrac{1}{R}\dfrac{\partial\sigma^{S^+}_{\theta z}}{\partial\theta} - \dfrac{\partial\sigma^{S^-}_{xz}}{\partial x} - \dfrac{1}{R}\dfrac{\partial\sigma^{S^-}_{\theta z}}{\partial\theta}}{2} + \frac{\dfrac{\partial\sigma^{S^+}_{xz}}{\partial x} + \dfrac{1}{R}\dfrac{\partial\sigma^{S^+}_{\theta z}}{\partial\theta} - \dfrac{\partial\sigma^{S^-}_{xz}}{\partial x} - \dfrac{1}{R}\dfrac{\partial\sigma^{S^-}_{\theta z}}{\partial\theta}}{h}z, \tag{8}$$

where S^+ and S^- denote the outer and inner surface layers of the nanoshell, respectively.

By inserting Eq. (7) into Eq. (8), it yields

$$\sigma_{zz} = \frac{2\tau_{\rm s}z}{h}\Big(\frac{\partial^2 w}{\partial x^2} + \frac{1}{R^2}\frac{\partial^2 w}{\partial\theta^2}\Big). \tag{9}$$

As a result, substituting Eq. (9) into Eq. (4) gives

$$\begin{pmatrix}\sigma_{xx}\\ \sigma_{\theta\theta}\end{pmatrix} = \begin{pmatrix}\lambda + 2\mu & \lambda\\ \lambda & \lambda + 2\mu\end{pmatrix}\begin{pmatrix}\varepsilon_{xx}\\ \varepsilon_{\theta\theta}\end{pmatrix} + \frac{\nu}{1-\nu}\begin{pmatrix}\sigma_{xx}\\ \sigma_{zz}\end{pmatrix}. \tag{10}$$

Thereby, the total strain energy of a nanoshell within the framework of the surface theory of elasticity can be written as follows:

$$\begin{aligned} \Pi_{\rm S} =& \frac{1}{2}\int_S\int_{-\frac{h}{2}}^{\frac{h}{2}}\sigma_{ij}\varepsilon_{ij}{\rm d}z{\rm d}S + \frac{1}{2}\Big(\int_{S^+}\sigma^S_{ij}\varepsilon_{ij}{\rm d}S^+ + \int_{S^-}\sigma^S_{ij}\varepsilon_{ij}{\rm d}S^-\Big)\\ =& \frac{1}{2}\int_S\Big(\overline{N}_{xx}\varepsilon^0_{xx} + \overline{N}_{\theta\theta}\varepsilon^0_{\theta\theta} + \overline{N}_{x\theta}\gamma^0_{x\theta} + \overline{M}_{xx}\kappa_{xx}\\ &+ \overline{M}_{\theta\theta}\kappa_{\theta\theta} + \overline{M}_{x\theta}\kappa_{\theta} + Q^S_x\frac{\partial w}{\partial x} + \frac{Q^S_\theta}{R}\frac{\partial w}{\partial\theta}\Big){\rm d}S, \end{aligned} \tag{11}$$

where the stress resultants can be achieved in the following forms:

$$\begin{cases} \overline{N}_{xx} = N_{xx} + \sigma_{xx}^{S^+} + \sigma_{xx}^{S^-} = A_{11}^* \varepsilon_{xx}^0 + A_{12}^* \varepsilon_{\theta\theta}^0 + 2\tau_{\mathrm{s}} - \tau_{\mathrm{s}} \Big(\dfrac{\partial w}{\partial x}\Big)^2, \\ \overline{N}_{\theta\theta} = N_{\theta\theta} + \sigma_{\theta\theta}^{S^+} + \sigma_{\theta\theta}^{S^-} = A_{11}^* \varepsilon_{\theta\theta}^0 + A_{12}^* \varepsilon_{xx}^0 + \dfrac{2\tau_{\mathrm{s}}}{R} w + 2\tau_{\mathrm{s}} - \tau_{\mathrm{s}} \Big(\dfrac{1}{R}\dfrac{\partial w}{\partial \theta}\Big)^2, \\ \overline{N}_{x\theta} = N_{x\theta} + \dfrac{1}{2}(\sigma_{x\theta}^{S^+} + \sigma_{x\theta}^{S^-} + \sigma_{\theta x}^{S^+} + \sigma_{\theta x}^{S^-}) = A_{55}^* \gamma_{x\theta}^0 - \dfrac{\tau_{\mathrm{s}}}{R}\dfrac{\partial w}{\partial x}\dfrac{\partial w}{\partial \theta}, \\ \overline{M}_{xx} = M_{xx} + \dfrac{h}{2}(\sigma_{xx}^{S^+} + \sigma_{xx}^{S^-}) = D_{11}^* \kappa_{xx} + D_{12}^* \kappa_{\theta\theta} + E_{11}^* \Big(\dfrac{\partial^2 w}{\partial x^2} + \dfrac{1}{R^2}\dfrac{\partial^2 w}{\partial \theta^2}\Big), \\ \overline{M}_{\theta\theta} = M_{\theta\theta} + \dfrac{h}{2}(\sigma_{\theta\theta}^{S^+} + \sigma_{\theta\theta}^{S^-}) = D_{11}^* \kappa_{\theta\theta} + D_{12}^* \kappa_{xx} + E_{11}^* \Big(\dfrac{\partial^2 w}{\partial x^2} + \dfrac{1}{R^2}\dfrac{\partial^2 w}{\partial \theta^2}\Big), \\ \overline{M}_{x\theta} = M_{x\theta} + \dfrac{h}{4}(\sigma_{x\theta}^{S^+} + \sigma_{x\theta}^{S^-} + \sigma_{\theta x}^{S^+} + \sigma_{\theta x}^{S^-}) = D_{55}^* \kappa_{x\theta}, \\ Q_x^S = \sigma_{xz}^{S^+} + \sigma_{xz}^{S^-} = 2\tau_{\mathrm{s}} \dfrac{\partial w}{\partial x}, \\ Q_\theta^S = \sigma_{\theta z}^{S^+} + \sigma_{\theta z}^{S^-} = \dfrac{2\tau_{\mathrm{s}}}{R}\dfrac{\partial w}{\partial \theta}, \end{cases} \tag{12}$$

where

$$\begin{pmatrix} N_{xx} \\ N_{\theta\theta} \\ N_{x\theta} \end{pmatrix} = \int_{-\frac{h}{2}}^{\frac{h}{2}} \begin{pmatrix} \sigma_{xx} \\ \sigma_{\theta\theta} \\ \sigma_{x\theta} \end{pmatrix} \mathrm{d}z, \quad \begin{pmatrix} M_{xx} \\ M_{\theta\theta} \\ M_{x\theta} \end{pmatrix} = \int_{-\frac{h}{2}}^{\frac{h}{2}} \begin{pmatrix} \sigma_{xx} \\ \sigma_{\theta\theta} \\ \sigma_{x\theta} \end{pmatrix} z \mathrm{d}z, \tag{13}$$

$$\begin{cases} A_{11}^* = (\lambda + 2\mu)h + 2(\lambda_{\mathrm{s}} + \mu_{\mathrm{s}}), \quad A_{12}^* = \lambda h + 2\tau_x + 2\lambda_{\mathrm{s}}, \\ A_{55}^* = \mu h + 2\mu_{\mathrm{s}} - \tau_{\mathrm{s}}, \quad D_{11}^* = \dfrac{(\lambda + 2\mu)h^3}{12} + \dfrac{(\lambda_{\mathrm{s}} + 2\mu_{\mathrm{s}})h^2}{2}, \\ D_{12}^* = \dfrac{\lambda h^3}{12} + \dfrac{(\lambda_{\mathrm{s}} + \tau_{\mathrm{s}})h^2}{2}, \quad D_{55}^* = \dfrac{\mu h^3}{12} + \dfrac{(2\mu_{\mathrm{s}} - \tau_{\mathrm{s}})h^2}{4}, \quad E_{11}^* = \dfrac{\nu h^2 \tau_{\mathrm{s}}}{6(1-\nu)}. \end{cases} \tag{14}$$

On the other hand, the kinetic energy of a nanoshell modeled based upon the surface elasticity theory can be given as

$$\begin{aligned} \Pi_{\mathrm{T}} &= \frac{1}{2}\int_S \Big((\rho h + 2\rho_{\mathrm{s}})\Big(\Big(\frac{\partial u_1}{\partial t}\Big)^2 + \Big(\frac{\partial u_2}{\partial t}\Big)^2 + \Big(\frac{\partial u_3}{\partial t}\Big)^2\Big)\Big)\mathrm{d}S \\ &= \frac{1}{2}\int_S \Big((\rho h + 2\rho_{\mathrm{s}})(\dot{u}^2 + \dot{v}^2 + \dot{w}^2) + \Big(\frac{\rho h^3}{12} + \frac{\rho_{\mathrm{s}} h^2}{6}\Big)\Big(\Big(\frac{\partial \dot{w}}{\partial x}\Big)^2 + \Big(\frac{1}{R}\frac{\partial \dot{w}}{\partial \theta}\Big)^2\Big)\Big)\mathrm{d}S, \end{aligned} \tag{15}$$

where ρ_{s} is the surface density, and the dot symbol indicates the time derivative.

Moreover, the work done by the external harmonic excitation can be calculated as

$$\Pi_{\mathrm{P}} = \int_S (F_u u + F_v v + F_w w)\,\mathrm{d}S. \tag{16}$$

On the basis of Hamilton's principle, one will have

$$\delta \int_{t_1}^{t_2} (\Pi_{\mathrm{T}} - \Pi_{\mathrm{S}} + \Pi_{\mathrm{P}})\mathrm{d}t = 0. \tag{17}$$

As a result, it yields

$$\begin{cases} \dfrac{\partial \overline{N}_{xx}}{\partial x}+\dfrac{1}{R}\dfrac{\partial \overline{N}_{x\theta}}{\partial \theta}-F_u=I_0\ddot{u}, \\ \dfrac{1}{R}\dfrac{\partial \overline{N}_{\theta\theta}}{\partial \theta}+\dfrac{\partial \overline{N}_{x\theta}}{\partial x}-F_v=I_0\ddot{v}, \\ \dfrac{\partial}{\partial x}\Big(\overline{N}_{xx}\dfrac{\partial w}{\partial x}\Big)+\dfrac{\overline{N}_{\theta\theta}}{R}+\dfrac{1}{R^2}\dfrac{\partial}{\partial \theta}\Big(\overline{N}_{\theta\theta}\dfrac{\partial w}{\partial \theta}\Big)+\dfrac{1}{R}\dfrac{\partial}{\partial x}\Big(\overline{N}_{x\theta}\dfrac{\partial w}{\partial \theta}\Big)+\dfrac{1}{R}\dfrac{\partial}{\partial \theta}\Big(\overline{N}_{x\theta}\dfrac{\partial w}{\partial x}\Big) \\ +\dfrac{\partial^2 \overline{M}_{xx}}{\partial x^2}+\dfrac{1}{R^2}\dfrac{\partial^2 \overline{M}_{\theta\theta}}{\partial \theta^2}+\dfrac{2}{R^2}\dfrac{\partial^2 \overline{M}_{x\theta}}{\partial x\partial \theta}+\dfrac{\partial Q_x^S}{\partial x}+\dfrac{1}{R}\dfrac{\partial Q_\theta^S}{\partial \theta}-F_w=I_0\ddot{w}-I_2\dfrac{\partial^2 \ddot{w}}{\partial x^2}-\dfrac{I_2}{R^2}\dfrac{\partial^2 \ddot{w}}{\partial \theta^2}, \end{cases} \tag{18}$$

where

$$I_0=\rho h+2\rho_{\rm s},\quad I_2=\frac{\rho h^3}{12}+\frac{\rho_{\rm s}h^2}{6}.$$

Also, the relevant size-dependent boundary conditions are extracted as

$$\begin{cases} \delta u=0 \quad \text{or} \quad \delta(\overline{N}_{xx})=0, \\ \delta v=0 \quad \text{or} \quad \delta\Big(\dfrac{1}{R}\overline{N}_{\theta\theta}\Big)=0, \\ \delta w=0 \quad \text{or} \quad \delta\Big(\overline{N}_{xx}\dfrac{\partial w}{\partial x}-\dfrac{\overline{N}_{\theta\theta}}{R}\dfrac{\partial w}{\partial \theta}-2\dfrac{\partial^2 \overline{M}_{xx}}{\partial x^2}-\dfrac{2}{R^2}\dfrac{\partial^2 \overline{M}_{\theta\theta}}{\partial \theta^2}-\dfrac{4}{R}\dfrac{\partial^2 \overline{M}_{x\theta}}{\partial x\partial \theta}+Q_x^S+Q_\theta^S\Big)=0. \end{cases} \tag{19}$$

By neglecting the in-plane inertia and assuming this point that the external harmonic excitation is applied only along the z-axis, the Airy stress function can be introduced as follows:

$$N_{xx}=\frac{1}{R^2}\frac{\partial^2\varphi}{\partial\theta^2},\quad N_{\theta\theta}=\frac{\partial^2\varphi}{\partial x^2},\quad N_{x\theta}=-\frac{1}{R}\frac{\partial^2\varphi}{\partial x\partial\theta}. \tag{20}$$

Consequently, the mid-plane strain components can be expressed as

$$\begin{cases} \varepsilon_{xx}^0=-\Gamma_2\dfrac{\partial^2\varphi}{\partial x^2}+\dfrac{\Gamma_1}{R^2}\dfrac{\partial^2\varphi}{\partial\theta^2}+2\tau_{\rm s}\Gamma_2\dfrac{w}{R}-\dfrac{2\tau_{\rm s}}{A_{11}^*+A_{12}^*}+\Gamma_1\tau_{\rm s}\Big(\dfrac{\partial w}{\partial x}\Big)^2-\Gamma_2\tau_{\rm s}\Big(\dfrac{1}{R}\dfrac{\partial w}{\partial\theta}\Big)^2, \\ \varepsilon_{\theta\theta}^0=-\dfrac{\Gamma_2}{R^2}\dfrac{\partial^2\varphi}{\partial\theta^2}+\Gamma_1\dfrac{\partial^2\varphi}{\partial x^2}-2\tau_{\rm s}\Gamma_1\dfrac{w}{R}-\dfrac{2\tau_{\rm s}}{A_{11}^*+A_{12}^*}+\Gamma_1\tau_{\rm s}\Big(\dfrac{1}{R}\dfrac{\partial w}{\partial\theta}\Big)^2-\Gamma_2\tau_{\rm s}\Big(\dfrac{\partial w}{\partial x}\Big)^2, \\ \gamma_{x\theta}^0=-\dfrac{\Gamma_3}{R}\dfrac{\partial^2\varphi}{\partial x\partial\theta}+\Gamma_3\dfrac{\tau_{\rm s}}{R}\dfrac{\partial w}{\partial x}\dfrac{\partial w}{\partial\theta}, \end{cases} \tag{21}$$

where

$$\Gamma_1=\frac{A_{11}^*}{\Big(A_{11}^*\Big)^2-\Big(A_{12}^*\Big)^2},\quad \Gamma_2=\frac{A_{12}^*}{\Big(A_{11}^*\Big)^2-\Big(A_{12}^*\Big)^2},\quad \Gamma_3=\frac{1}{A_{55}^*}. \tag{22}$$

According to geometrical compatibility, for a shell-type structure, one will have

$$\frac{1}{R^2}\frac{\partial^2\varepsilon_{xx}^0}{\partial\theta^2}+\frac{\partial^2\varepsilon_{\theta\theta}^0}{\partial x^2}-\frac{1}{R}\frac{\partial^2\gamma_{x\theta}^0}{\partial x\partial\theta}=\Big(\frac{1}{R}\frac{\partial^2\gamma_{x\theta}^0}{\partial x\partial\theta}\Big)^2-\frac{1}{R^2}\frac{\partial^2 w}{\partial x^2}\frac{\partial^2 w}{\partial\theta^2}-\frac{1}{R}\frac{\partial^2 w}{\partial x^2}. \tag{23}$$

Through inserting Eqs. (12) and (21) into Eqs. (18) and (23), the governing differential equations of motion for a nanoshell modeled via the surface theory of elasticity under a soft harmonic

excitation are obtained as

$$\begin{cases} \Gamma_4\dfrac{\partial^4 w}{\partial x^4}+\dfrac{2\Gamma_5}{R^2}\dfrac{\partial^4 w}{\partial x^2\partial\theta^2}+\dfrac{\Gamma_4}{R^4}\dfrac{\partial^4 w}{\partial\theta^4}-2\tau_{\rm s}\dfrac{\partial^2 w}{\partial x^2}-\dfrac{2\tau_{\rm s}}{R^2}\dfrac{\partial^2 w}{\partial\theta^2}+I_0\ddot{w}-I_2\dfrac{\partial^2\ddot{w}}{\partial x^2}-\dfrac{I_2}{R^2}\dfrac{\partial^2\ddot{w}}{\partial\theta^2} \\ \quad =F_w+\dfrac{\partial^2\varphi}{\partial x^2}+\dfrac{1}{R^2}\Big(\dfrac{\partial^2 w}{\partial\theta^2}\dfrac{\partial^2\varphi}{\partial x^2}-2\dfrac{\partial^2 w}{\partial x\partial\theta}\dfrac{\partial^2\varphi}{\partial x\partial\theta}+\dfrac{\partial^2 w}{\partial x^2}\dfrac{\partial^2\varphi}{\partial\theta^2}\Big), \\ \Gamma_1\dfrac{\partial^4\varphi}{\partial x^4}+\dfrac{(\Gamma_3-2\Gamma_2)}{R^2}\dfrac{\partial^4\varphi}{\partial x^2\partial\theta^2}+\dfrac{\Gamma_1}{R^4}\dfrac{\partial^4\varphi}{\partial\theta^4} \\ \quad =\dfrac{1}{R^2}\Big(\dfrac{\partial^2 w}{\partial x\partial\theta}\Big)^2-\dfrac{1}{R^2}\dfrac{\partial^2 w}{\partial x^2}\dfrac{\partial^2 w}{\partial\theta^2}-\dfrac{1}{R}\dfrac{\partial^2 w}{\partial x^2}+\dfrac{2\tau_{\rm s}}{R}\Big(\Gamma_1\dfrac{\partial^2 w}{\partial x^2}-\dfrac{\Gamma_2}{R^2}\dfrac{\partial^2 w}{\partial\theta^2}\Big) \\ \qquad -\dfrac{2\tau_{\rm s}\Gamma_1}{R^2}\Big(\dfrac{\partial^3 w}{\partial x\partial\theta^2}\dfrac{\partial w}{\partial x}+2\Big(\dfrac{\partial^2 w}{\partial x\partial\theta}\Big)^2+\dfrac{\partial^3 w}{\partial x^2\partial\theta}\dfrac{\partial w}{\partial\theta}\Big) \\ \qquad +2\tau_{\rm s}\Gamma_2\Big(\dfrac{\partial^3 w}{\partial x^3}\dfrac{\partial w}{\partial x}+\dfrac{1}{R^4}\dfrac{\partial^3 w}{\partial\theta^3}\dfrac{\partial w}{\partial\theta}+\Big(\dfrac{\partial^2 w}{\partial x^2}\Big)^2+\Big(\dfrac{1}{R^2}\dfrac{\partial^2 w}{\partial\theta^2}\Big)^2\Big) \\ \qquad +\dfrac{\tau_{\rm s}\Gamma_3}{R^2}\Big(\dfrac{\partial^3 w}{\partial x^2\partial\theta}\dfrac{\partial w}{\partial\theta}+\dfrac{\partial^2 w}{\partial x^2}\dfrac{\partial^2 w}{\partial\theta^2}+\Big(\dfrac{\partial^2 w}{\partial x\partial\theta}\Big)^2+\dfrac{\partial w}{\partial x}\dfrac{\partial^3 w}{\partial x\partial\theta^2}\Big), \end{cases} \tag{24}$$

where

$$\Gamma_4=D_{11}^*-E_{11}^*,\quad \Gamma_5=D_{12}^*+2D_{55}^*-E_{11}^*. \tag{25}$$

3 Multi-time-scale solving process

To capture the solution of the problem in a more general form, the following dimensionless parameters are taken into account:

$$\begin{cases} X=\dfrac{x}{L},\quad W=\dfrac{w}{h},\quad U=\dfrac{u}{L},\quad V=\dfrac{v}{R},\quad (a_{11}^*,a_{12}^*,a_{55}^*)=\Big(\dfrac{A_{11}^*}{A_{110}},\dfrac{A_{12}^*}{A_{110}},\dfrac{A_{55}^*}{A_{110}}\Big), \\ \overline{\tau}_{\rm s}=\dfrac{\tau_{\rm s}}{A_{110}},\quad \phi=\dfrac{\varphi}{A_{110}h^2},\quad (d_{11}^*,d_{12}^*,d_{55}^*,e_{11}^*)=\Big(\dfrac{D_{11}^*}{A_{110}h^2},\dfrac{D_{12}^*}{A_{110}h^2},\dfrac{D_{55}^*}{A_{110}h^2},\dfrac{E_{11}^*}{A_{110}h^2}\Big), \\ I_0^*=\dfrac{I_0}{I_{10}},\quad I_2^*=\dfrac{I_2}{I_{10}h^2},\quad \xi=\dfrac{R}{L},\quad \eta=\dfrac{h}{R},\quad T=\dfrac{t}{L}\sqrt{\dfrac{A_{110}}{I_{10}}},\quad f_w=\dfrac{F_wL^2}{A_{110}h}, \end{cases} \tag{26}$$

where $A_{110}=(\lambda+2\mu)h$, and $I_{10}=\rho h$.

As a result, the dimensionless form of Eq. (24) can be expressed as

$$\begin{aligned} &\overline{\Gamma}_4\xi^2\eta^2\frac{\partial^4 W}{\partial X^4}+2\overline{\Gamma}_5\eta^2\frac{\partial^4 W}{\partial X^2\partial\theta^2}+\frac{\overline{\Gamma}_4\eta^2}{\xi^2}\frac{\partial^4 W}{\partial\theta^4}-2\overline{\tau}_{\rm s}\frac{\partial^2 W}{\partial X^2}-\frac{2\overline{\tau}_{\rm s}}{\xi^2}\frac{\partial^2 W}{\partial\theta^2} \\ &\quad +I_0^*\frac{\partial^2 W}{\partial T^2}-I_2^*\xi^2\eta^2\frac{\partial^4 W}{\partial X^2\partial T^2}-I_2^*\eta^2\frac{\partial^4 W}{\partial\theta^2\partial T^2} \\ &=f_w+\eta\frac{\partial^2\phi}{\partial X^2}+\eta^2\Big(\frac{\partial^2 W}{\partial\theta^2}\frac{\partial^2\phi}{\partial X^2}-2\frac{\partial^2 W}{\partial X\partial\theta}\frac{\partial^2\phi}{\partial X\partial\theta}+\frac{\partial^2 W}{\partial X^2}\frac{\partial^2\phi}{\partial\theta^2}\Big), \end{aligned} \tag{27a}$$

$$
\begin{aligned}
&\overline{\Gamma}_1\xi^2\eta^2\frac{\partial^4\phi}{\partial X^4}+\Big(\overline{\Gamma}_3-2\overline{\Gamma}_2\Big)\eta^2\frac{\partial^4\phi}{\partial X^2\partial\theta^2}+\frac{\overline{\Gamma}_1\eta^2}{\xi^2}\frac{\partial^4\phi}{\partial\theta^4}\\
&=\eta^2\Big(\frac{\partial^2W}{\partial X\partial\theta}\Big)^2-\eta^2\frac{\partial^2W}{\partial X^2}\frac{\partial^2W}{\partial\theta^2}-\eta\frac{\partial^2W}{\partial X^2}+2\overline{\tau}_{\rm s}\Big(\overline{\Gamma}_1\eta\frac{\partial^2W}{\partial X^2}-\frac{\overline{\Gamma}_2\eta}{\xi^2}\frac{\partial^2W}{\partial\theta^2}\Big)\\
&\quad-2\overline{\tau}_{\rm s}\overline{\Gamma}_1\eta^2\Big(\frac{\partial^3W}{\partial X\partial\theta^2}\frac{\partial W}{\partial X}+2\Big(\frac{\partial^2W}{\partial X\partial\theta}\Big)^2+\frac{\partial^3W}{\partial X^2\partial\theta}\frac{\partial W}{\partial\theta}\Big)\\
&\quad+2\overline{\tau}_{\rm s}\overline{\Gamma}_2\Big(\frac{\partial^3W}{\partial X^3}\frac{\partial W}{\partial X}+\frac{\eta^2}{\xi^2}\frac{\partial^3W}{\partial\theta^3}\frac{\partial W}{\partial\theta}+\eta^2\xi^2\Big(\frac{\partial^2W}{\partial X^2}\Big)^2+\frac{\eta^2}{\xi^2}\Big(\frac{\partial^2W}{\partial\theta^2}\Big)^2\Big)\\
&\quad+\overline{\tau}_{\rm s}\overline{\Gamma}_3\Big(\frac{\partial^3W}{\partial X^2\partial\theta}\frac{\partial W}{\partial\theta}+\frac{\partial^2W}{\partial X^2}\frac{\partial^2W}{\partial\theta^2}+\Big(\frac{\partial^2W}{\partial X\partial\theta}\Big)^2+\frac{\partial W}{\partial X}\frac{\partial^3W}{\partial X\partial\theta^2}\Big),
\end{aligned}
\tag{27b}
$$

where

$$
\begin{cases}
\overline{\Gamma}_1=\dfrac{a_{11}^*}{(a_{11}^*)^2-(a_{12}^*)^2},\quad \overline{\Gamma}_2=\dfrac{a_{12}^*}{(a_{11}^*)^2-(a_{12}^*)^2},\quad \overline{\Gamma}_3=\dfrac{1}{a_{55}^*},\\
\overline{\Gamma}_4=d_{11}^*-e_{11}^*,\quad \overline{\Gamma}_5=d_{12}^*+2d_{55}^*-e_{11}^*.
\end{cases}
\tag{28}
$$

In order to analyze the nonlinear vibration response of shell-type structures, several expansions have been proposed for the lateral deflection. Refs. [42] and [43] have demonstrated that in order to capture accurate and practical results, it is necessary to consider the companion mode in addition to the simple linear vibration mode. On the other hand, those modes which lead to convergence of the answer are the symmetric modes. As a result, in this work, the following expansion is assumed for the lateral deflection of a nanoshell:

$$
W(X,\theta)=A_{1,n}\cos(n\theta)\sin(\pi X)+A_{1,0}\sin(\pi X)+A_{3,0}\sin(3\pi X)+A_{5,0}\sin(5\pi X).
\tag{29}
$$

Also, based upon the Weaver and Unny theory, the harmonic external excitation can be modeled in the following form[42–43]:

$$
F_w(x,\theta,t)=f_n\cos(n\theta)\sin\Big(\frac{\pi x}{L}\Big)\cos(\Omega t).
\tag{30}
$$

By inserting Eq. (29) into Eq. (27b), the geometrical compatibility is satisfied. Accordingly, the solution for the variable of ϕ can be expressed via the summation of the homogenous and particular parts as below

$$
\phi=\phi_{\rm h}+\phi_{\rm p},
\tag{31}
$$

where the particular part of the solution can be given as

$$
\begin{aligned}
\phi_{\rm p}=&c_1(t)\cos(n\theta)\sin(\pi X)+c_2(t)\sin(\pi X)+c_3(t)\sin(3\pi X)+c_4(t)\sin(5\pi X)\\
&+c_5(t)\cos(2\pi X)+c_6(t)\cos(n\theta)+c_7(t)\cos(n\theta)\cos(2\pi X)\\
&+c_8(t)\cos(n\theta)\cos(4\pi X)+c_9(t)\cos(n\theta)\cos(6\pi X)+c_{10}(t)\cos(2n\theta).
\end{aligned}
\tag{32}
$$

The parameters of $c_i(t), i=1,2,\cdots,10$, are presented in Appendix A.

The homogeneous part of the solution is extracted in such a way that the following conditions are satisfied completely[42–43]:

$$
\begin{cases}
\dfrac{1}{2\pi}\displaystyle\int_0^{2\pi}\int_0^1\frac{\partial V}{\partial\theta}{\rm d}X{\rm d}\theta=0,\\
\widetilde{N}_{xx}=\dfrac{1}{2\pi}\displaystyle\int_0^{2\pi}\int_0^1\overline{N}_{xx}^*{\rm d}X{\rm d}\theta=0,\\
\widetilde{N}_{x\theta}=\dfrac{1}{2\pi}\displaystyle\int_0^{2\pi}\int_0^1\overline{N}_{x\theta}^*{\rm d}X{\rm d}\theta=0,
\end{cases}
\tag{33}
$$

where

$$\begin{cases} \overline{N}^*_{xx} = a^*_{11}\Big(\dfrac{\partial U}{\partial X} + \dfrac{1}{2}\xi^2\eta^2\Big(\dfrac{\partial W}{\partial X}\Big)^2\Big) + a^*_{12}\Big(\dfrac{\partial V}{\partial \theta} - \eta W + \dfrac{1}{2}\eta^2\Big(\dfrac{\partial W}{\partial \theta}\Big)^2\Big), \\ \overline{N}^*_{x\theta} = a^*_{55}\Big(\dfrac{1}{\xi}\dfrac{\partial U}{\partial \theta} + \xi\dfrac{\partial V}{\partial X} + \eta^2\xi\dfrac{\partial W}{\partial X}\dfrac{\partial W}{\partial \theta}\Big). \end{cases} \tag{34}$$

Also, one will have

$$\phi_{\rm h} = \frac{1}{2}X^2\Big(\overline{N}^*_{\theta\theta} - \frac{1}{2\pi}\int_0^{2\pi}\int_0^1 \frac{\partial^2\phi_{\rm p}}{\partial X^2}{\rm d}X{\rm d}\theta\Big), \tag{35}$$

where

$$\overline{N}^*_{\theta\theta} = a^*_{11}\Big(\frac{\partial V}{\partial \theta} - \eta W + \frac{1}{2}\eta^2\Big(\frac{\partial W}{\partial \theta}\Big)^2\Big) + a^*_{12}\Big(\frac{\partial U}{\partial X} + \frac{1}{2}\xi^2\eta^2\Big(\frac{\partial W}{\partial X}\Big)^2\Big). \tag{36}$$

By using Eqs. (12) and (35), one will have

$$\widetilde{N}_{\theta\theta} = \frac{1}{2\pi}\int_0^{2\pi}\int_0^1 \Big(\frac{1}{2}\frac{\eta^2}{\overline{\Gamma}_1}\Big(\frac{\partial W}{\partial \theta}\Big)^2 - \frac{\eta}{\overline{\Gamma}_1}W\Big){\rm d}X{\rm d}\theta. \tag{37}$$

Substituting Eq. (29) into Eq. (37), and then integrating within the associated limitations yield

$$\widetilde{N}_{\theta\theta} = \frac{n^2\eta^2}{8\overline{\Gamma}_1}A^2_{1,n} - \frac{2\eta}{\pi\overline{\Gamma}_1}\Big(A_{1,0} + \frac{A_{3,0}}{3} + \frac{A_{5,0}}{5}\Big). \tag{38}$$

By inserting Eqs. (32), (33), and (38) into Eq. (35), the homogeneous part of the solution can be extracted as

$$\phi_{\rm h} = \frac{1}{2}X^2\Big(\frac{n^2\eta^2}{8\overline{\Gamma}_1}A^2_{1,n}\Big). \tag{39}$$

Now, the obtained solution for the Airy stress function is substituted in Eq. (27a) which results in a general equation with three unknown parameters as unknown general coordinates. In order to continue the solving process, the Galerkin technique is put to use including orthogonal basis functions as follows:

$$g_s(X,\theta) = \begin{cases} \cos(n\theta)\sin(\pi X) & \text{for} \quad s = 1, \\ \sin(\pi X) & \text{for} \quad s = 2, \\ \sin(3\pi X) & \text{for} \quad s = 3, \\ \sin(5\pi X) & \text{for} \quad s = 4. \end{cases} \tag{40}$$

As a result, the following four coupled ordinary differential equations are acquired:

$$\begin{cases} \ddot{A}_{1,n} + \omega^2_{1,n}A_{1,n} + \alpha_1 A^3_{1,n} + \alpha_2 A_{1,n}A_{1,0} + \alpha_3 A_{1,n}A_{3,0} + \alpha_4 A_{1,n}A_{5,0} \\ \quad + \alpha_5 A_{1,n}A^2_{1,0} + \alpha_6 A_{1,n}A^2_{3,0} + \alpha_7 A_{1,n}A^2_{5,0} \\ \quad + \alpha_8 A_{1,n}A_{1,0}A_{3,0} + \alpha_9 A_{1,n}A_{3,0}A_{5,0} = f_n\cos(\Omega t), \\ \ddot{A}_{1,0} + \omega^2_{1,0}A_{1,0} + \beta_1 A^2_{1,n} + \beta_2 A_{1,0}A^2_{1,n} + \beta_3 A_{3,0}A^2_{1,n} = 0, \\ \ddot{A}_{3,0} + \omega^2_{3,0}A_{3,0} + \vartheta_1 A^2_{1,n} + \vartheta_2 A_{1,0}A^2_{1,n} + \vartheta_3 A_{3,0}A^2_{1,n} + \vartheta_4 A_{5,0}A^2_{1,n} = 0, \\ \ddot{A}_{5,0} + \omega^2_{5,0}A_{5,0} + \psi_1 A^2_{1,n} + \psi_2 A_{3,0}A^2_{1,n} + \psi_3 A_{5,0}A^2_{1,n} = 0, \end{cases} \tag{41}$$

where α_i, β_i, ϑ_i, and ψ_i are constants as functions of the material properties and geometrical parameters.

In order to achieve the solution to the problem in a more general form, the following dimensionless parameters are defined:

$$\begin{cases} q_1 = A_{1,n}, \quad q_2 = A_{1,0}, \quad q_3 = A_{3,0}, \quad q_4 = A_{5,0}, \\ \widetilde{f}_n = \dfrac{f_n}{\widehat{\omega}_{1,n}^2}, \quad \widehat{t} = \widehat{\omega}_{1,n} t, \end{cases} \tag{42}$$

where $\widehat{\omega}_{1,n}$ represents the value of $\omega_{1,n}$ without consideration of the surface free energy effect.

As a consequence, Eq. (41) can be rewritten in the dimensionless form as follows:

$$\begin{cases} \ddot{q}_1 + \omega_0^2 q_1 + \overline{\alpha}_1 q_1^3 + \overline{\alpha}_2 q_1 q_2 + \overline{\alpha}_3 q_1 q_3 + \overline{\alpha}_4 q_1 q_4 \\ \quad + \overline{\alpha}_5 q_1 q_2^2 + \overline{\alpha}_6 q_1 q_3^2 + \overline{\alpha}_7 q_1 q_4^2 + \overline{\alpha}_8 q_1 q_2 q_3 + \overline{\alpha}_9 q_1 q_3 q_4 = \widetilde{f}_n \cos(\widetilde{\Omega}\widehat{t}), \\ \ddot{q}_2 + \omega_1^2 q_2 + \overline{\beta}_1 q_1^2 + \overline{\beta}_2 q_2 q_1^2 + \overline{\beta}_3 q_3 q_1^2 = 0, \\ \ddot{q}_3 + \omega_3^2 q_3 + \overline{\vartheta}_1 q_1^2 + \overline{\vartheta}_2 q_2 q_1^2 + \overline{\vartheta}_3 q_3 q_1^2 + \overline{\vartheta}_4 q_4 q_1^2 = 0, \\ \ddot{q}_4 + \omega_5^2 q_4 + \overline{\psi}_1 q_1^2 + \overline{\psi}_2 q_3 q_1^2 + \overline{\psi}_3 q_4 q_1^2 = 0, \end{cases} \tag{43}$$

where

$$\begin{cases} (\omega_0, \omega_1, \omega_3, \omega_5, \widetilde{\Omega}) = \Big(\dfrac{\omega_{1,n}}{\widehat{\omega}_{1,n}}, \dfrac{\omega_{1,0}}{\widehat{\omega}_{1,n}} \dfrac{\omega_{3,0}}{\widehat{\omega}_{1,n}} \dfrac{\omega_{5,0}}{\widehat{\omega}_{1,n}} \dfrac{\Omega}{\widehat{\omega}_{1,n}}\Big), \\ \big(\overline{\alpha}_2, \overline{\alpha}_3, \overline{\alpha}_4, \overline{\beta}_1, \overline{\vartheta}_1, \overline{\psi}_1\big) = \Big(\dfrac{\alpha_2}{\widehat{\omega}_{1,n}^2}, \dfrac{\alpha_3}{\widehat{\omega}_{1,n}^2}, \dfrac{\alpha_4}{\widehat{\omega}_{1,n}^2}, \dfrac{\beta_1}{\widehat{\omega}_{1,n}^2}, \dfrac{\vartheta_1}{\widehat{\omega}_{1,n}^2}, \dfrac{\psi_1}{\widehat{\omega}_{1,n}^2}\Big), \\ (\overline{\alpha}_1, \overline{\alpha}_5, \overline{\alpha}_6, \overline{\alpha}_7, \overline{\alpha}_8, \overline{\alpha}_9) = \Big(\dfrac{\alpha_1}{\widehat{\omega}_{1,n}^2}, \dfrac{\alpha_5}{\widehat{\omega}_{1,n}^2}, \dfrac{\alpha_6}{\widehat{\omega}_{1,n}^2}, \dfrac{\alpha_7}{\widehat{\omega}_{1,n}^2}, \dfrac{\alpha_8}{\widehat{\omega}_{1,n}^2}, \dfrac{\alpha_9}{\widehat{\omega}_{1,n}^2}\Big), \\ \big(\overline{\beta}_2, \overline{\beta}_3, \overline{\vartheta}_2, \overline{\vartheta}_3, \overline{\vartheta}_4, \overline{\psi}_2, \overline{\psi}_3\big) = \Big(\dfrac{\beta_2}{\widehat{\omega}_{1,n}^2}, \dfrac{\beta_3}{\widehat{\omega}_{1,n}^2}, \dfrac{\vartheta_2}{\widehat{\omega}_{1,n}^2}, \dfrac{\vartheta_3}{\widehat{\omega}_{1,n}^2}, \dfrac{\vartheta_4}{\widehat{\omega}_{1,n}^2}, \dfrac{\psi_2}{\widehat{\omega}_{1,n}^2}, \dfrac{\psi_3}{\widehat{\omega}_{1,n}^2}\Big). \end{cases} \tag{44}$$

3.1 Solution for the main vibration mode

In this case, only the terms related to the main vibration mode are considered and the other ones are ignored. Therefore, it yields only one differential equation of motion as follows:

$$\ddot{q}_1 + 2\varepsilon\xi_{1,n}\omega_0\dot{q}_1 + \omega_0^2 q_1 + \varepsilon\overline{\alpha}_1 q_1^3 = \varepsilon\widetilde{f}_n \cos(\widetilde{\Omega}\,\widehat{t}), \tag{45}$$

where ε denotes the scaling parameter to scale the nonlinear terms, damping, and external excitation. Also, in accordance with the Rayleigh dissipation function, the damping is assumed as a function of the linear frequency of the system.

Now, with the aid of the multi-time-scale method, it is assumed that

$$q_1(T_0, T_1) = q_{10}(T_0, T_1) + \varepsilon q_{11}(T_0, T_1), \tag{46}$$

where $T_0 = \widehat{t}$ and $T_1 = \varepsilon\widehat{t}$ denote different time scales.

On the other hand, the perturbation of the excitation frequency around the linear frequency of the system is taken into account as below,

$$\widetilde{\Omega} = \omega_0 + \varepsilon\eta, \tag{47}$$

where η is the detuning parameter.

Through inserting Eqs. (46) and (47) into Eq. (45) and employing the multi-time-scale technique, the following set of equations are obtained:

$$\begin{cases} \varepsilon^0 \ \rightarrow \ D_0^2 q_{10} + \omega_0^2 q_{10} = 0, \\ \varepsilon^1 \ \rightarrow \ D_0^2 q_{11} + \omega_0^2 q_{11} = -2D_0 D_1 q_{10} - \overline{\alpha}_1 q_{10}^2 + \widetilde{f}_n \cos(\omega_0 T_0 + \eta T_1), \end{cases} \tag{48}$$

where $D_i^j = \dfrac{\mathrm{d}^j}{\mathrm{d}T_i^j}$ are various orders of time derivative.

The solution to the first part of the set of Eq. (48) can be expressed as

$$q_{10} = A\mathrm{e}^{\mathrm{i}\omega_0 T_0} + \overline{A}\mathrm{e}^{-\mathrm{i}\omega_0 T_0}, \tag{49}$$

where A is a complex function of T_0 and T_1. Also, $\overline{A}$ stands for the complex conjugate of A.

Substitution of Eq. (49) into the second part of the set of Eq. (48) leads to the following differential equation:

$$\begin{aligned} D_0^2 q_{11} + \omega_0^2 q_{11} = & -\Big(2\mathrm{i}\omega_0\Big(\frac{\partial A}{\partial T_1} + \xi_{1,n}\omega_0 A\Big) + 3\overline{\alpha}_1 A^2 \overline{A}\Big)\mathrm{e}^{\mathrm{i}\omega_0 T_0} - \overline{\alpha}_1 A^3 \mathrm{e}^{3\mathrm{i}\omega_0 T_0} \\ & + \frac{1}{2}\widetilde{f}_n \mathrm{e}^{\mathrm{i}(\omega_0 T_0 + \eta T_1)} + \mathrm{C.C.}, \end{aligned} \tag{50}$$

where the term of C.C. represents the complex conjugate of its previous expressions.

To eliminate the secular terms, one will have

$$2\mathrm{i}\omega_0\Big(\frac{\partial A}{\partial T_1} + \xi_{1,n}\omega_0 A\Big) + 3\overline{\alpha}_1 A^2 \overline{A} + \frac{1}{2}\widetilde{f}_n \mathrm{e}^{\mathrm{i}\eta T_1} = 0. \tag{51}$$

Polar functions are assumed for $A(T_0, T_1)$ as follows:

$$A(T_1) = \frac{1}{2}a(T_1)\mathrm{e}^{\mathrm{i}\varsigma(T_1)}. \tag{52}$$

By inserting Eq. (52) into Eq. (51), each of the real and imaginary parts gives

$$\begin{cases} \dfrac{\mathrm{d}a}{\mathrm{d}T_1} = -\xi_{1,n}\omega_0 a - \dfrac{1}{2\omega_0}\sin(\eta T_1 - \varsigma), \\ a\dfrac{\mathrm{d}\varsigma}{\mathrm{d}T_1} = \dfrac{3\overline{\alpha}_1}{8\omega_0}a^3 - \dfrac{1}{2\omega_0}\cos(\eta T_1 - \varsigma). \end{cases} \tag{53}$$

In order to extract the steady-state solution, the derivative terms on the left side of Eq. (53) are set to be zero. Consequently, it yields

$$\begin{cases} \xi_{1,n}\omega_0 a = \dfrac{1}{2\omega_0}\sin(\eta T_1 - \varsigma), \\ \eta a - \dfrac{3\overline{\alpha}_1}{8\omega_0}a^3 = -\dfrac{1}{2\omega_0}\cos(\eta T_1 - \varsigma). \end{cases} \tag{54}$$

As a result, one will have

$$\eta = \frac{3\overline{\alpha}_1 a^2}{8\omega_0} \pm \sqrt{\frac{\widetilde{f}_n^2}{4a^2\omega_0^2} - \xi_{1,n}^2\omega_0^2}. \tag{55}$$

3.2 Solution for the interaction of the main and first symmetric vibration modes

In order to enhance the accuracy of the resonance solution, at the first step, the interaction of the only first symmetric vibration mode with the main one is taken into consideration. Therefore, it gives

$$\begin{cases} \ddot{q}_1 + 2\varepsilon^2\xi_{1,n}\omega_0\dot{q}_1 + \omega_0^2 q_1 + \varepsilon^2\overline{\alpha}_1 q_1^3 + \varepsilon\overline{\alpha}_2 q_1 q_2 + \varepsilon^2\overline{\alpha}_5 q_1 q_2^2 = \varepsilon^2 \widetilde{f}_n \cos(\widetilde{\Omega}\,\widehat{t}), \\ \ddot{q}_2 + 2\varepsilon^2\xi_{1,0}\omega_1\dot{q}_2 + \omega_1^2 q_2 + \varepsilon\overline{\beta}_1 q_1^2 + \varepsilon^2\overline{\beta}_2 q_2 q_1^2 = 0. \end{cases} \tag{56}$$

To apply the multi-time-scale method, it is supposed that

$$\begin{cases} q_1(T_0,T_1,T_2) = q_{10}(T_0,T_1,T_2) + \varepsilon q_{11}(T_0,T_1,T_2) + \varepsilon^2 q_{12}(T_0,T_1,T_2), \\ q_2(T_0,T_1,T_2) = q_{20}(T_0,T_1,T_2) + \varepsilon q_{21}(T_0,T_1,T_2) + \varepsilon^2 q_{22}(T_0,T_1,T_2), \\ \widetilde{\Omega} = \omega_0 + \varepsilon^2\eta, \end{cases} \tag{57}$$

where $T_2 = \varepsilon^2\widehat{t}$.

By inserting Eq. (57) into Eq. (56) and employing the multi-time-scale technique, the sets of equations corresponding to different orders of ε are obtained which are presented in Appendix B.

The associated solution can be written as

$$\begin{cases} D_0^2 q_{12} + \omega_0^2 q_{12} = -2\mathrm{i}\omega_0\dfrac{\partial A}{\partial T_2}\mathrm{e}^{\mathrm{i}\omega_0 T_0} - 2\mathrm{i}\xi_{1,n}\omega_0^2 A\mathrm{e}^{\mathrm{i}\omega_0 T_0} - 3\overline{\alpha}_1 A^2\overline{A}\mathrm{e}^{\mathrm{i}\omega_0 T_0} \\ \qquad - \dfrac{\overline{\alpha}_2\overline{\beta}_1}{4\omega_0^2-\omega_1^2}A^2\overline{A}\mathrm{e}^{\mathrm{i}\omega_0 T_0} + \dfrac{2\overline{\alpha}_2\overline{\beta}_1}{\omega_1^2}A^2\overline{A}\mathrm{e}^{\mathrm{i}\omega_0 T_0} \\ \qquad - \dfrac{\overline{\alpha}_2^2}{(\omega_1+\omega_0)^2-1}AB\overline{B}\mathrm{e}^{\mathrm{i}\omega_0 T_0} - \dfrac{\overline{\alpha}_2^2}{(\omega_1-\omega_0)^2-1}AB\overline{B}\mathrm{e}^{\mathrm{i}\omega_0 T_0} \\ \qquad - \overline{\alpha}_5 AB\overline{B}\mathrm{e}^{\mathrm{i}\omega_0 T_0} + \dfrac{1}{2}\widetilde{f}_n\mathrm{e}^{\mathrm{i}(\omega_0 T_0+\eta T_2)} + \text{N.S.T.} + \text{C.C.}, \\ D_0^2 q_{22} + \omega_1^2 q_{22} = -2\mathrm{i}\omega_1\dfrac{\partial B}{\partial T_2}\mathrm{e}^{\mathrm{i}\omega_1 T_0} - 2\mathrm{i}\xi_{1,0}\omega_1^2 B\mathrm{e}^{\mathrm{i}\omega_1 T_0} - \dfrac{2\overline{\alpha}_2\overline{\beta}_1}{(\omega_1+\omega_0)^2-1}A\overline{A}B\mathrm{e}^{\mathrm{i}\omega_1 T_0} \\ \qquad - \dfrac{2\overline{\alpha}_2\overline{\beta}_1}{(\omega_1-\omega_0)^2-1}A\overline{A}B\mathrm{e}^{\mathrm{i}\omega_1 T_0} - \overline{\beta}_2 A\overline{A}B\mathrm{e}^{\mathrm{i}\omega_1 T_0} + \text{N.S.T.} + \text{C.C.}, \end{cases} \tag{58}$$

where N.S.T. represents the non-secular terms.

Through the elimination of the secular terms, it yields

$$\begin{cases} -2\mathrm{i}\omega_0\dfrac{\partial A}{\partial T_2} - 2\mathrm{i}\xi_{1,n}\omega_0^2 A - 3\overline{\alpha}_1 A^2\overline{A} - \dfrac{\overline{\alpha}_2\overline{\beta}_1}{4\omega_0^2-\omega_1^2}A^2\overline{A} + \dfrac{2\overline{\alpha}_2\overline{\beta}_1}{\omega_1^2}A^2\overline{A} - \dfrac{\overline{\alpha}_2^2}{(\omega_1+\omega_0)^2-1}AB\overline{B} \\ -\dfrac{\overline{\alpha}_2^2}{(\omega_1-\omega_0)^2-1}AB\overline{B} - \overline{\alpha}_5 AB\overline{B} + \dfrac{1}{2}\widetilde{f}_n\mathrm{e}^{\mathrm{i}\eta T_2} = 0, \\ -2\mathrm{i}\omega_1\dfrac{\partial B}{\partial T_2} - 2\mathrm{i}\xi_{1,0}\omega_1^2 B - \dfrac{2\overline{\alpha}_2\overline{\beta}_1}{(\omega_1+\omega_0)^2-1}A\overline{A}B - \dfrac{2\overline{\alpha}_2\overline{\beta}_1}{(\omega_1-\omega_0)^2-1}A\overline{A}B - \overline{\beta}_2 A\overline{A}B = 0. \end{cases} \tag{59}$$

Polar functions are assumed for $A(T_2)$ and $B(T_2)$ as follows:

$$A(T_2) = \frac{1}{2}a(T_2)\mathrm{e}^{\mathrm{i}\varsigma(T_2)}, \quad B(T_2) = \frac{1}{2}b(T_2)\mathrm{e}^{\mathrm{i}\zeta(T_2)}. \tag{60}$$

Substitution of Eq. (60) into Eq. (59) leads to the following relationships:

$$\begin{cases} -\dfrac{\mathrm{d}a}{\mathrm{d}T_2} - \xi_{1,n}\omega_0 a + \dfrac{1}{2\omega_0}\widetilde{f}_n \sin(\eta T_2 - \varsigma) = 0, \\ a\dfrac{\mathrm{d}\varsigma}{\mathrm{d}T_2} - \dfrac{3\overline{\alpha}_1}{8\omega_0}a^3 - \dfrac{\overline{\alpha}_2\overline{\beta}_1}{4\omega_0\omega_1^2}a^3 - \dfrac{\overline{\alpha}_2^2}{8\omega_0((\omega_1+\omega_0)^2-1)}ab^2 \\ -\dfrac{\overline{\alpha}_2^2}{8\omega_0((\omega_1-\omega_0)^2-1)}ab^2 - \dfrac{\overline{\alpha}_5}{8\omega_0}ab^2 + \dfrac{1}{2\omega_0}f_n\cos(\eta T_2 - \varsigma) = 0, \\ -\dfrac{\mathrm{d}b}{\mathrm{d}T_2} - \xi_{1,0}\omega_1 b = 0, \\ b\dfrac{\mathrm{d}\zeta}{\mathrm{d}T_2} - \dfrac{\overline{\alpha}_2\overline{\beta}_1}{4\omega_1((\omega_1+\omega_0)^2-1)}a^2 b - \dfrac{\overline{\alpha}_2\overline{\beta}_1}{4\omega_1((\omega_1-\omega_0)^2-1)}a^2 b - \dfrac{\overline{\beta}_2}{8\omega_1}a^2 b = 0. \end{cases} \tag{61}$$

In order to extract the steady-state solution, the derivative terms in Eq. (61) are set to be zero. As a consequence, one will have

$$\begin{cases} \xi_{1,n}\omega_0 a = \dfrac{1}{2\omega_0}\widetilde{f}_n \sin(\eta T_2 - \varsigma), \\ \eta a - \dfrac{3\overline{\alpha}_1}{8\omega_0}a^3 - \dfrac{\overline{\alpha}_2\overline{\beta}_1}{8\omega_0(4\omega_0^2-\omega_1^2)}a^3 + \dfrac{\overline{\alpha}_2\overline{\beta}_1}{4\omega_0\omega_1^2}a^3 = -\dfrac{1}{2\omega_0}\widetilde{f}_n\cos(\eta T_2 - \varsigma). \end{cases} \tag{62}$$

Therefore, it can be concluded that

$$\eta = \Big(\frac{3\overline{\alpha}_1}{8\omega_0} + \frac{\overline{\alpha}_2\overline{\beta}_1}{8\omega_0(4\omega_0^2-\omega_1^2)} - \frac{\overline{\alpha}_2\overline{\beta}_1}{4\omega_0\omega_1^2}\Big)a^2 \pm \sqrt{\frac{\widetilde{f}_n^2}{4a^2\omega_0^2} - \xi_{1,n}^2\omega_0^2}. \tag{63}$$

3.3 Solution for the interaction of the main, first, and third symmetric vibration modes

In order to achieve more accuracy, the interactions of the first and third symmetric vibration modes with the main one are taken into consideration. Therefore, it gives

$$\begin{cases} \ddot{q}_1 + 2\varepsilon^2\xi_{1,n}\omega_0\dot{q}_1 + \omega_0^2 q_1 + \varepsilon^2\overline{\alpha}_1 q_1^3 + \varepsilon\overline{\alpha}_2 q_1 q_2 + \varepsilon\overline{\alpha}_3 q_1 q_3 + \varepsilon^2\overline{\alpha}_5 q_1 q_2^2 + \varepsilon^2\overline{\alpha}_6 q_1 q_3^2 \\ \quad + \varepsilon^2\overline{\alpha}_8 q_1 q_2 q_3 = \varepsilon^2\widetilde{f}_n\cos(\widetilde{\Omega}\widehat{t}), \\ \ddot{q}_2 + 2\varepsilon^2\xi_{1,0}\omega_1\dot{q}_2 + \omega_1^2 q_2 + \varepsilon\overline{\beta}_1 q_1^2 + \varepsilon^2\overline{\beta}_2 q_2 q_1^2 + \varepsilon^2\overline{\beta}_3 q_3 q_1^2 = 0, \\ \ddot{q}_3 + 2\varepsilon^2\xi_{3,0}\omega_3\dot{q}_3 + \omega_3^2 q_3 + \varepsilon\overline{\vartheta}_1 q_1^2 + \varepsilon^2\overline{\vartheta}_2 q_2 q_1^2 + \varepsilon^2\overline{\vartheta}_3 q_3 q_1^2 = 0. \end{cases} \tag{64}$$

To apply the multi-time-scale method, it is supposed that

$$\begin{cases} q_1(T_0,T_1,T_2) = q_{10}(T_0,T_1,T_2) + \varepsilon q_{11}(T_0,T_1,T_2) + \varepsilon^2 q_{12}(T_0,T_1,T_2), \\ q_2(T_0,T_1,T_2) = q_{20}(T_0,T_1,T_2) + \varepsilon q_{21}(T_0,T_1,T_2) + \varepsilon^2 q_{22}(T_0,T_1,T_2), \\ q_3(T_0,T_1,T_2) = q_{30}(T_0,T_1,T_2) + \varepsilon q_{31}(T_0,T_1,T_2) + \varepsilon^2 q_{32}(T_0,T_1,T_2), \\ \widetilde{\Omega} = \omega_0 + \varepsilon^2\eta. \end{cases} \tag{65}$$

By inserting Eq. (65) into Eq. (64) and employing the multi-time-scale technique, the sets of equations corresponding to different orders of ε are obtained which are given in Appendix B.

The associated solution can be expressed as

$$
\begin{cases}
D_0^2 q_{12} + \omega_0^2 q_{12} = -2\mathrm{i}\omega_0 \dfrac{\partial A}{\partial T_2}\mathrm{e}^{\mathrm{i}\omega_0 T_0} - 2\mathrm{i}\xi_{1,n}\omega_0^2 A\mathrm{e}^{\mathrm{i}\omega_0 T_0} - 3\overline{\alpha}_1 A^2\overline{A}\mathrm{e}^{\mathrm{i}\omega_0 T_0} \\
\qquad\qquad - \dfrac{\overline{\alpha}_2\overline{\beta}_1}{4\omega_0^2-\omega_1^2}A^2\overline{A}\mathrm{e}^{\mathrm{i}\omega_0 T_0} + \dfrac{2\overline{\alpha}_2\overline{\beta}_1}{\omega_1^2}A^2\overline{A}\mathrm{e}^{\mathrm{i}\omega_0 T_0} \\
\qquad\qquad - \dfrac{\overline{\alpha}_2^2}{(\omega_1+\omega_0)^2-1}AB\overline{B}\mathrm{e}^{\mathrm{i}\omega_0 T_0} - \dfrac{\overline{\alpha}_2^2}{(\omega_1-\omega_0)^2-1}AB\overline{B}\mathrm{e}^{\mathrm{i}\omega_0 T_0} \\
\qquad\qquad - \dfrac{\overline{\alpha}_3\overline{\vartheta}_1}{4\omega_0^2-\omega_3^2}A^2\overline{A}\mathrm{e}^{\mathrm{i}\omega_0 T_0} + \dfrac{2\overline{\alpha}_3\overline{\vartheta}_1}{\omega_3^2}A^2\overline{A}\mathrm{e}^{\mathrm{i}\omega_0 T_0} \\
\qquad\qquad - \dfrac{\overline{\alpha}_3^2}{(\omega_3+\omega_0)^2-1}AC\overline{C}\mathrm{e}^{\mathrm{i}\omega_0 T_0} - \dfrac{\overline{\alpha}_3^2}{(\omega_3-\omega_0)^2-1}AC\overline{C}\mathrm{e}^{\mathrm{i}\omega_0 T_0} \\
\qquad\qquad - \overline{\alpha}_5 AB\overline{B}\mathrm{e}^{\mathrm{i}\omega_0 T_0} - \overline{\alpha}_6 AC\overline{C}\mathrm{e}^{\mathrm{i}\omega_0 T_0} + \dfrac{1}{2}\widetilde{f}_n\mathrm{e}^{\mathrm{i}(\omega_0 T_0+\eta T_2)} + \text{N.S.T.} + \text{C.C.}, \\
D_0^2 q_{22} + \omega_1^2 q_{22} = -2\mathrm{i}\omega_1 \dfrac{\partial B}{\partial T_2}\mathrm{e}^{\mathrm{i}\omega_1 T_0} - 2\mathrm{i}\xi_{1,0}\omega_1^2 B\mathrm{e}^{\mathrm{i}\omega_1 T_0} - \dfrac{2\overline{\alpha}_2\overline{\beta}_1}{(\omega_1+\omega_0)^2-1}A\overline{A}B\mathrm{e}^{\mathrm{i}\omega_1 T_0} \\
\qquad\qquad - \dfrac{2\overline{\alpha}_2\overline{\beta}_1}{(\omega_1-\omega_0)^2-1}A\overline{A}B\mathrm{e}^{\mathrm{i}\omega_1 T_0} - \overline{\beta}_2 A\overline{A}B\mathrm{e}^{\mathrm{i}\omega_1 T_0} + \text{N.S.T.} + \text{C.C.}, \\
D_0^2 q_{32} + \omega_3^2 q_{32} = -2\mathrm{i}\omega_3 \dfrac{\partial C}{\partial T_2}\mathrm{e}^{\mathrm{i}\omega_3 T_0} - 2\mathrm{i}\xi_{3,0}\omega_3^2 C\mathrm{e}^{\mathrm{i}\omega_3 T_0} - \dfrac{2\overline{\alpha}_3\overline{\vartheta}_1}{(\omega_3+\omega_0)^2-1}A\overline{A}C\mathrm{e}^{\mathrm{i}\omega_3 T_0} \\
\qquad\qquad - \dfrac{2\overline{\alpha}_3\overline{\vartheta}_1}{(\omega_3-\omega_0)^2-1}A\overline{A}C\mathrm{e}^{\mathrm{i}\omega_3 T_0} - \overline{\vartheta}_2 A\overline{A}C\mathrm{e}^{\mathrm{i}\omega_3 T_0} + \text{N.S.T.} + \text{C.C.}
\end{cases}
\tag{66}
$$

Through the elimination of the secular terms, it yields

$$
\begin{cases}
-2\mathrm{i}\omega_0\dfrac{\partial A}{\partial T_2} - 2\mathrm{i}\xi_{1,n}\omega_0^2 A - 3\overline{\alpha}_1 A^2\overline{A} - \dfrac{\overline{\alpha}_2\overline{\beta}_1}{4\omega_0^2-\omega_1^2}A^2\overline{A} + \dfrac{2\overline{\alpha}_2\overline{\beta}_1}{\omega_1^2}A^2\overline{A} - \dfrac{\overline{\alpha}_2^2}{(\omega_1+\omega_0)^2-1}AB\overline{B} \\
-\dfrac{\overline{\alpha}_2^2}{(\omega_1-\omega_0)^2-1}AB\overline{B} - \dfrac{\overline{\alpha}_3\overline{\vartheta}_1}{4\omega_0^2-\omega_3^2}A^2\overline{A} + \dfrac{2\overline{\alpha}_3\overline{\vartheta}_1}{\omega_3^2}A^2\overline{A} - \dfrac{\overline{\alpha}_3^2}{(\omega_3+\omega_0)^2-1}AC\overline{C} \\
-\dfrac{\overline{\alpha}_3^2}{(\omega_3-\omega_0)^2-1}AC\overline{C} - \overline{\alpha}_5 AB\overline{B} - \overline{\alpha}_6 AC\overline{C} + \dfrac{1}{2}\widetilde{f}_n\mathrm{e}^{\mathrm{i}\eta T_2} = 0, \\
-2\mathrm{i}\omega_1\dfrac{\partial B}{\partial T_2} - 2\mathrm{i}\xi_{1,0}\omega_1^2 B - \dfrac{2\overline{\alpha}_2\overline{\beta}_1}{(\omega_1+\omega_0)^2-1}A\overline{A}B - \dfrac{2\overline{\alpha}_2\overline{\beta}_1}{(\omega_1-\omega_0)^2-1}A\overline{A}B - \overline{\beta}_2 A\overline{A}B = 0, \\
-2\mathrm{i}\omega_3\dfrac{\partial C}{\partial T_2} - 2\mathrm{i}\xi_{3,0}\omega_3^2 C - \dfrac{2\overline{\alpha}_3\overline{\vartheta}_1}{(\omega_3+\omega_0)^2-1}A\overline{A}C - \dfrac{2\overline{\alpha}_3\overline{\vartheta}_1}{(\omega_3-\omega_0)^2-1}A\overline{A}C - \overline{\vartheta}_2 A\overline{A}C = 0.
\end{cases}
\tag{67}
$$

Polar functions are assumed for $A(T_2)$, $B(T_2)$, and $C(T_2)$ as follows:

$$
A(T_2) = \frac{1}{2}a(T_2)\mathrm{e}^{\mathrm{i}\varsigma(T_2)}, \quad B(T_2) = \frac{1}{2}b(T_2)\mathrm{e}^{\mathrm{i}\zeta(T_2)}, \quad C(T_2) = \frac{1}{2}c(T_2)\mathrm{e}^{\mathrm{i}\chi(T_2)}. \tag{68}
$$

Substitution of Eq. (68) into Eq. (67) leads to the following relationships:

$$\begin{cases} -\dfrac{\mathrm{d}a}{\mathrm{d}T_2} - \xi_{1,n}\omega_0 a + \dfrac{1}{2\omega_0}\widetilde{f}_n \sin(\eta T_2 - \varsigma) = 0, \\ a\dfrac{\mathrm{d}\varsigma}{\mathrm{d}T_2} - \dfrac{3\overline{\alpha}_1}{8\omega_0}a^3 - \dfrac{\overline{\alpha}_2\overline{\beta}_1}{8\omega_0(4\omega_0^2-\omega_1^2)}a^3 + \dfrac{\overline{\alpha}_2\overline{\beta}_1}{4\omega_0\omega_1^2}a^3 - \dfrac{\overline{\alpha}_3\overline{\vartheta}_1}{8\omega_0(4\omega_0^2-\omega_3^2)}a^3 + \dfrac{\overline{\alpha}_3\overline{\vartheta}_1}{4\omega_0\omega_3^2}a^3 \\ -\dfrac{\overline{\alpha}_2^2}{8\omega_0((\omega_1+\omega_0)^2-1)}ab^2 - \dfrac{\overline{\alpha}_2^2}{8\omega_0((\omega_1-\omega_0)^2-1)}ab^2 \\ -\dfrac{\overline{\alpha}_3^2}{8\omega_0((\omega_3+\omega_0)^2-1)}ac^2 - \dfrac{\overline{\alpha}_3^2}{8\omega_0((\omega_3-\omega_0)^2-1)}ac^2 \\ -\dfrac{\overline{\alpha}_5}{8\omega_0}ab^2 - \dfrac{\overline{\alpha}_6}{8\omega_0}ac^2 + \dfrac{1}{2\omega_0}f_n\cos(\eta T_2 - \varsigma) = 0, \\ -\dfrac{\mathrm{d}b}{\mathrm{d}T_2} - \xi_{1,0}\omega_1 b = 0, \\ b\dfrac{\mathrm{d}\zeta}{\mathrm{d}T_2} - \dfrac{\overline{\alpha}_2\overline{\beta}_1}{4\omega_1((\omega_1+\omega_0)^2-1)}a^2b - \dfrac{\overline{\alpha}_2\overline{\beta}_1}{4\omega_1((\omega_1-\omega_0)^2-1)}a^2b - \dfrac{\overline{\beta}_2}{8\omega_1}a^2b = 0, \\ -\dfrac{\mathrm{d}c}{\mathrm{d}T_2} - \xi_{3,0}\omega_3 c = 0, \\ c\dfrac{\mathrm{d}\chi}{\mathrm{d}T_2} - \dfrac{\overline{\alpha}_3\overline{\vartheta}_1}{4\omega_3((\omega_3+\omega_0)^2-1)}a^2c - \dfrac{\overline{\alpha}_3\overline{\vartheta}_1}{4\omega_3((\omega_3-\omega_0)^2-1)}a^2c - \dfrac{\overline{\vartheta}_2}{8\omega_3}a^2c = 0. \end{cases} \tag{69}$$

In order to extract the steady-state solution, the derivative terms in Eq. (69) are set to zero. As a consequence, one will have

$$\begin{cases} \xi_{1,n}\omega_0 a = \dfrac{1}{2\omega_0}\widetilde{f}_n \sin(\eta T_2 - \varsigma), \\ \eta a - \dfrac{3\overline{\alpha}_1}{8\omega_0}a^3 - \dfrac{\overline{\alpha}_2\overline{\beta}_1}{8\omega_0(4\omega_0^2-\omega_1^2)}a^3 + \dfrac{\overline{\alpha}_2\overline{\beta}_1}{4\omega_0\omega_1^2}a^3 - \dfrac{\overline{\alpha}_3\overline{\vartheta}_1}{8\omega_0(4\omega_0^2-\omega_3^2)}a^3 + \dfrac{\overline{\alpha}_3\overline{\vartheta}_1}{4\omega_0\omega_3^2}a^3 \\ = -\dfrac{1}{2\omega_0}\widetilde{f}_n\cos(\eta T_2 - \varsigma). \end{cases} \tag{70}$$

Therefore, it can be concluded that

$$\eta = \Big(\frac{3\overline{\alpha}_1}{8\omega_0} + \frac{\overline{\alpha}_2\overline{\beta}_1}{8\omega_0(4\omega_0^2-\omega_1^2)} - \frac{\overline{\alpha}_2\overline{\beta}_1}{4\omega_0\omega_1^2} + \frac{\overline{\alpha}_3\overline{\vartheta}_1}{8\omega_0(4\omega_0^2-\omega_3^2)} - \frac{\overline{\alpha}_3\overline{\vartheta}_1}{4\omega_0\omega_3^2}\Big)a^2 \pm \sqrt{\frac{\widetilde{f}_n^2}{4a^2\omega_0^2} - \xi_{1,n}^2\omega_0^2}. \tag{71}$$

3.4 Solution for the interaction of the main, first, third, and fifth symmetric vibration modes

In order to achieve more accuracy, the interactions of the first, third, and fifth symmetric vibration modes with the main one are taken into consideration. Therefore, it results in

$$\begin{cases} \ddot{q}_1 + 2\varepsilon^2\xi_{1,n}\omega_0\dot{q}_1 + \omega_0^2 q_1 + \varepsilon^2\overline{\alpha}_1 q_1^3 + \varepsilon\overline{\alpha}_2 q_1 q_2 + \varepsilon\overline{\alpha}_3 q_1 q_3 + \varepsilon\overline{\alpha}_4 q_1 q_4 + \varepsilon^2\overline{\alpha}_5 q_1 q_2^2 \\ \quad + \varepsilon^2\overline{\alpha}_6 q_1 q_3^2 + \varepsilon^2\overline{\alpha}_7 q_1 q_4^2 + \varepsilon^2\overline{\alpha}_8 q_1 q_2 q_3 + \varepsilon^2\overline{\alpha}_9 q_1 q_3 q_4 = \varepsilon^2\widetilde{f}_n\cos(\widetilde{\Omega}\,\widehat{t}), \\ \ddot{q}_2 + 2\varepsilon^2\xi_{1,0}\omega_1\dot{q}_2 + \omega_1^2 q_2 + \varepsilon\overline{\beta}_1 q_1^2 + \varepsilon^2\overline{\beta}_2 q_2 q_1^2 + \varepsilon^2\overline{\beta}_3 q_3 q_1^2 = 0, \\ \ddot{q}_3 + 2\varepsilon^2\xi_{3,0}\omega_3\dot{q}_3 + \omega_3^2 q_3 + \varepsilon\overline{\vartheta}_1 q_1^2 + \varepsilon^2\overline{\vartheta}_2 q_2 q_1^2 + \varepsilon^2\overline{\vartheta}_3 q_3 q_1^2 + \varepsilon^2\overline{\vartheta}_4 q_4 q_1^2 = 0, \\ \ddot{q}_4 + 2\varepsilon^2\xi_{5,0}\omega_5\dot{q}_4 + \omega_5^2 q_4 + \varepsilon\overline{\psi}_1 q_1^2 + \varepsilon^2\overline{\psi}_2 q_2 q_1^2 + \varepsilon^2\overline{\psi}_3 q_4 q_1^2 = 0. \end{cases} \tag{72}$$

To apply the multi-time-scale method, it is supposed that

$$\begin{cases} q_1(T_0,T_1,T_2) = q_{10}(T_0,T_1,T_2) + \varepsilon q_{11}(T_0,T_1,T_2) + \varepsilon^2 q_{12}(T_0,T_1,T_2), \\ q_2(T_0,T_1,T_2) = q_{20}(T_0,T_1,T_2) + \varepsilon q_{21}(T_0,T_1,T_2) + \varepsilon^2 q_{22}(T_0,T_1,T_2), \\ q_3(T_0,T_1,T_2) = q_{30}(T_0,T_1,T_2) + \varepsilon q_{31}(T_0,T_1,T_2) + \varepsilon^2 q_{32}(T_0,T_1,T_2), \\ q_4(T_0,T_1,T_2) = q_{40}(T_0,T_1,T_2) + \varepsilon q_{41}(T_0,T_1,T_2) + \varepsilon^2 q_{42}(T_0,T_1,T_2), \\ \widetilde{\Omega} = \omega_0 + \varepsilon^2 \eta. \end{cases} \tag{73}$$

By inserting Eq. (73) into Eq. (72) and employing the multi-time-scale technique, the sets of equations corresponding to different orders of ε are obtained as presented in Appendix B. The associated solution can be written as

$$\begin{cases} D_0^2 q_{12} + \omega_0^2 q_{12} = -2\mathrm{i}\omega_0 \dfrac{\partial A}{\partial T_2}\mathrm{e}^{\mathrm{i}\omega_0 T_0} - 2\mathrm{i}\xi_{1,n}\omega_0^2 A\mathrm{e}^{\mathrm{i}\omega_0 T_0} - 3\overline{\alpha}_1 A^2\overline{A}\mathrm{e}^{\mathrm{i}\omega_0 T_0} \\ \qquad - \dfrac{\overline{\alpha}_2\overline{\beta}_1}{4\omega_0^2-\omega_1^2}A^2\overline{A}\mathrm{e}^{\mathrm{i}\omega_0 T_0} + \dfrac{2\overline{\alpha}_2\overline{\beta}_1}{\omega_1^2}A^2\overline{A}\mathrm{e}^{\mathrm{i}\omega_0 T_0} \\ \qquad - \dfrac{\overline{\alpha}_2^2}{(\omega_1+\omega_0)^2-1}AB\overline{B}\mathrm{e}^{\mathrm{i}\omega_0 T_0} - \dfrac{\overline{\alpha}_2^2}{(\omega_1-\omega_0)^2-1}AB\overline{B}\mathrm{e}^{\mathrm{i}\omega_0 T_0} \\ \qquad - \dfrac{\overline{\alpha}_3\overline{\vartheta}_1}{4\omega_0^2-\omega_3^2}A^2\overline{A}\mathrm{e}^{\mathrm{i}\omega_0 T_0} + \dfrac{2\overline{\alpha}_3\overline{\vartheta}_1}{\omega_3^2}A^2\overline{A}\mathrm{e}^{\mathrm{i}\omega_0 T_0} \\ \qquad - \dfrac{\overline{\alpha}_3^2}{(\omega_3+\omega_0)^2-1}AC\overline{C}\mathrm{e}^{\mathrm{i}\omega_0 T_0} - \dfrac{\overline{\alpha}_3^2}{(\omega_3-\omega_0)^2-1}AC\overline{C}\mathrm{e}^{\mathrm{i}\omega_0 T_0} \\ \qquad - \dfrac{\overline{\alpha}_4\overline{\psi}_1}{4\omega_0^2-\omega_5^2}A^2\overline{A}\mathrm{e}^{\mathrm{i}\omega_0 T_0} + \dfrac{2\overline{\alpha}_4\overline{\psi}_1}{\omega_5^2}A^2\overline{A}\mathrm{e}^{\mathrm{i}\omega_0 T_0} \\ \qquad - \dfrac{\overline{\alpha}_4^2}{(\omega_5+\omega_0)^2-1}AF\overline{F}\mathrm{e}^{\mathrm{i}\omega_0 T_0} - \dfrac{\overline{\alpha}_4^2}{(\omega_5-\omega_0)^2-1}AF\overline{F}\mathrm{e}^{\mathrm{i}\omega_0 T_0} \\ \qquad - \overline{\alpha}_5 AB\overline{B}\mathrm{e}^{\mathrm{i}\omega_0 T_0} - \overline{\alpha}_6 AC\overline{C}\mathrm{e}^{\mathrm{i}\omega_0 T_0} - \overline{\alpha}_7 AF\overline{F}\mathrm{e}^{\mathrm{i}\omega_0 T_0} \\ \qquad + \dfrac{1}{2}\widetilde{f}_n\mathrm{e}^{\mathrm{i}(\omega_0 T_0+\eta T_2)} + \text{N.S.T.} + \text{C.C.}, \\ D_0^2 q_{22} + \omega_1^2 q_{22} = -2\mathrm{i}\omega_1 \dfrac{\partial B}{\partial T_2}\mathrm{e}^{\mathrm{i}\omega_1 T_0} - 2\mathrm{i}\xi_{1,0}\omega_1^2 B\mathrm{e}^{\mathrm{i}\omega_1 T_0} - \dfrac{2\overline{\alpha}_2\overline{\beta}_1}{(\omega_1+\omega_0)^2-1}A\overline{A}B\mathrm{e}^{\mathrm{i}\omega_1 T_0} \\ \qquad - \dfrac{2\overline{\alpha}_2\overline{\beta}_1}{(\omega_1-\omega_0)^2-1}A\overline{A}B\mathrm{e}^{\mathrm{i}\omega_1 T_0} - \overline{\beta}_2 A\overline{A}B\mathrm{e}^{\mathrm{i}\omega_1 T_0} + \text{N.S.T.} + \text{C.C.}, \\ D_0^2 q_{32} + \omega_3^2 q_{32} = -2\mathrm{i}\omega_3 \dfrac{\partial C}{\partial T_2}\mathrm{e}^{\mathrm{i}\omega_3 T_0} - 2\mathrm{i}\xi_{3,0}\omega_3^2 C\mathrm{e}^{\mathrm{i}\omega_3 T_0} - \dfrac{2\overline{\alpha}_3\overline{\vartheta}_1}{(\omega_3+\omega_0)^2-1}A\overline{A}C\mathrm{e}^{\mathrm{i}\omega_3 T_0} \\ \qquad - \dfrac{2\overline{\alpha}_3\overline{\vartheta}_1}{(\omega_3-\omega_0)^2-1}A\overline{A}C\mathrm{e}^{\mathrm{i}\omega_3 T_0} - \overline{\vartheta}_2 A\overline{A}C\mathrm{e}^{\mathrm{i}\omega_3 T_0} + \text{N.S.T.} + \text{C.C.}, \\ D_0^2 q_{42} + \omega_5^2 q_{42} = -2\mathrm{i}\omega_5 \dfrac{\partial F}{\partial T_2}\mathrm{e}^{\mathrm{i}\omega_5 T_0} - 2\mathrm{i}\xi_{5,0}\omega_5^2 F\mathrm{e}^{\mathrm{i}\omega_5 T_0} - \dfrac{2\overline{\alpha}_4\overline{\psi}_1}{(\omega_5+\omega_0)^2-1}A\overline{A}F\mathrm{e}^{\mathrm{i}\omega_5 T_0} \\ \qquad - \dfrac{2\overline{\alpha}_4\overline{\psi}_1}{(\omega_5-\omega_0)^2-1}A\overline{A}F\mathrm{e}^{\mathrm{i}\omega_5 T_0} - \overline{\psi}_2 A\overline{A}F\mathrm{e}^{\mathrm{i}\omega_5 T_0} + \text{N.S.T.} + \text{C.C.} \end{cases} \tag{74}$$

Through the elimination of the secular terms, it yields

$$\begin{cases} -2\mathrm{i}\omega_0\dfrac{\partial A}{\partial T_2}-2\mathrm{i}\xi_{1,n}\omega_0^2A-3\overline{\alpha}_1A^2\overline{A}-\dfrac{\overline{\alpha}_2\overline{\beta}_1}{4\omega_0^2-\omega_1^2}A^2\overline{A}+\dfrac{2\overline{\alpha}_2\overline{\beta}_1}{\omega_1^2}A^2\overline{A}-\dfrac{\overline{\alpha}_2^2}{(\omega_1+\omega_0)^2-1}AB\overline{B} \\ -\dfrac{\overline{\alpha}_2^2}{(\omega_1-\omega_0)^2-1}AB\overline{B}-\dfrac{\overline{\alpha}_3\overline{\vartheta}_1}{4\omega_0^2-\omega_3^2}A^2\overline{A}+\dfrac{2\overline{\alpha}_3\overline{\vartheta}_1}{\omega_3^2}A^2\overline{A}-\dfrac{\overline{\alpha}_3^2}{(\omega_3+\omega_0)^2-1}AC\overline{C} \\ -\dfrac{\overline{\alpha}_3^2}{(\omega_3-\omega_0)^2-1}AC\overline{C}-\dfrac{\overline{\alpha}_4\overline{\psi}_1}{4\omega_0^2-\omega_5^2}A^2\overline{A}+\dfrac{2\overline{\alpha}_4\overline{\psi}_1}{\omega_5^2}A^2\overline{A}-\dfrac{\overline{\alpha}_4^2}{(\omega_5+\omega_0)^2-1}AF\overline{F} \\ -\dfrac{\overline{\alpha}_4^2}{(\omega_5-\omega_0)^2-1}AF\overline{F}-\overline{\alpha}_5AB\overline{B}-\overline{\alpha}_6AC\overline{C}-\overline{\alpha}_7AF\overline{F}+\dfrac{1}{2}\widetilde{f}_n\mathrm{e}^{\mathrm{i}\eta T_2}=0, \\ -2\mathrm{i}\omega_1\dfrac{\partial B}{\partial T_2}-2\mathrm{i}\xi_{1,0}\omega_1^2B-\dfrac{2\overline{\alpha}_2\overline{\beta}_1}{(\omega_1+\omega_0)^2-1}A\overline{A}B-\dfrac{2\overline{\alpha}_2\overline{\beta}_1}{(\omega_1-\omega_0)^2-1}A\overline{A}B-\overline{\beta}_2A\overline{A}B=0, \\ -2\mathrm{i}\omega_3\dfrac{\partial C}{\partial T_2}-2\mathrm{i}\xi_{3,0}\omega_3^2C-\dfrac{2\overline{\alpha}_3\overline{\vartheta}_1}{(\omega_3+\omega_0)^2-1}A\overline{A}C-\dfrac{2\overline{\alpha}_3\overline{\vartheta}_1}{(\omega_3-\omega_0)^2-1}A\overline{A}C-\overline{\vartheta}_2A\overline{A}C=0, \\ -2\mathrm{i}\omega_5\dfrac{\partial F}{\partial T_2}-2\mathrm{i}\xi_{5,0}\omega_5^2F-\dfrac{2\overline{\alpha}_4\overline{\psi}_1}{(\omega_5+\omega_0)^2-1}A\overline{A}F-\dfrac{2\overline{\alpha}_4\overline{\psi}_1}{(\omega_5-\omega_0)^2-1}A\overline{A}F-\overline{\psi}_2A\overline{A}F=0. \end{cases} \tag{75}$$

Polar functions are assumed for $A(T_2)$, $B(T_2)$, $C(T_2)$, and $F(T_2)$ as follows:

$$\begin{cases} A(T_2)=\dfrac{1}{2}a(T_2)\mathrm{e}^{\mathrm{i}\varsigma(T_2)}, \quad B(T_2)=\dfrac{1}{2}b(T_2)\mathrm{e}^{\mathrm{i}\zeta(T_2)}, \\ C(T_2)=\dfrac{1}{2}c(T_2)\mathrm{e}^{\mathrm{i}\chi(T_2)}, \quad F(T_2)=\dfrac{1}{2}f(T_2)\mathrm{e}^{\mathrm{i}\delta(T_2)}. \end{cases} \tag{76}$$

Substitution of Eq. (76) into Eq. (75) leads to the following relationships:

$$\begin{cases} -\dfrac{\mathrm{d}a}{\mathrm{d}T_2}-\xi_{1,n}\omega_0a+\dfrac{1}{2\omega_0}\widetilde{f}_n\sin(\eta T_2-\varsigma)=0, \\ a\dfrac{\mathrm{d}\varsigma}{\mathrm{d}T_2}-\dfrac{3\overline{\alpha}_1}{8\omega_0}a^3-\dfrac{\overline{\alpha}_2\overline{\beta}_1}{8\omega_0(4\omega_0^2-\omega_1^2)}a^3+\dfrac{\overline{\alpha}_2\overline{\beta}_1}{4\omega_0\omega_1^2}a^3-\dfrac{\overline{\alpha}_3\overline{\vartheta}_1}{8\omega_0(4\omega_0^2-\omega_3^2)}a^3+\dfrac{\overline{\alpha}_3\overline{\vartheta}_1}{4\omega_0\omega_3^2}a^3 \\ -\dfrac{\overline{\alpha}_4\overline{\psi}_1}{8\omega_0(4\omega_0^2-\omega_5^2)}a^3+\dfrac{\overline{\alpha}_4\overline{\psi}_1}{4\omega_0\omega_5^2}a^3-\dfrac{\overline{\alpha}_2^2}{8\omega_0((\omega_1+\omega_0)^2-1)}ab^2 \\ -\dfrac{\overline{\alpha}_2^2}{8\omega_0((\omega_1-\omega_0)^2-1)}ab^2-\dfrac{\overline{\alpha}_3^2}{8\omega_0((\omega_3+\omega_0)^2-1)}ac^2 \\ -\dfrac{\overline{\alpha}_3^2}{8\omega_0((\omega_3-\omega_0)^2-1)}ac^2-\dfrac{\overline{\alpha}_4^2}{8\omega_0((\omega_5+\omega_0)^2-1)}af^2 \\ -\dfrac{\overline{\alpha}_4^2}{8\omega_0((\omega_5-\omega_0)^2-1)}af^2-\dfrac{\overline{\alpha}_5}{8\omega_0}ab^2-\dfrac{\overline{\alpha}_6}{8\omega_0}ac^2-\dfrac{\overline{\alpha}_7}{8\omega_0}af^2 \\ +\dfrac{1}{2\omega_0}f_n\cos(\eta T_2-\varsigma)=0, \\ -\dfrac{\mathrm{d}b}{\mathrm{d}T_2}-\xi_{1,0}\omega_1b=0, \\ b\dfrac{\mathrm{d}\zeta}{\mathrm{d}T_2}-\dfrac{\overline{\alpha}_2\overline{\beta}_1}{4\omega_1((\omega_1+\omega_0)^2-1)}a^2b-\dfrac{\overline{\alpha}_2\overline{\beta}_1}{4\omega_1((\omega_1-\omega_0)^2-1)}a^2b-\dfrac{\overline{\beta}_2}{8\omega_1}a^2b=0, \\ -\dfrac{\mathrm{d}c}{\mathrm{d}T_2}-\xi_{3,0}\omega_3c=0, \\ c\dfrac{\mathrm{d}\chi}{\mathrm{d}T_2}-\dfrac{\overline{\alpha}_3\overline{\vartheta}_1}{4\omega_3((\omega_3+\omega_0)^2-1)}a^2c-\dfrac{\overline{\alpha}_3\overline{\vartheta}_1}{4\omega_3((\omega_3-\omega_0)^2-1)}a^2c-\dfrac{\overline{\vartheta}_2}{8\omega_3}a^2c=0, \\ -\dfrac{\mathrm{d}f}{\mathrm{d}T_2}-\xi_{5,0}\omega_5f=0, \\ f\dfrac{\mathrm{d}\delta}{\mathrm{d}T_2}-\dfrac{\overline{\alpha}_4\overline{\psi}_1}{4\omega_5((\omega_5+\omega_0)^2-1)}a^2f-\dfrac{\overline{\alpha}_4\overline{\psi}_1}{4\omega_5((\omega_5-\omega_0)^2-1)}a^2f-\dfrac{\overline{\psi}_2}{8\omega_5}a^2f=0. \end{cases} \tag{77}$$

In order to extract the steady-state solution, the derivative terms in Eq. (77) are set to zero. As a consequence, one will have

$$\begin{cases} \xi_{1,n}\omega_0 a = \dfrac{1}{2\omega_0}\widetilde{f}_n \sin(\eta T_2 - \varsigma), \\ \eta a - \dfrac{3\overline{\alpha}_1}{8\omega_0}a^3 - \dfrac{\overline{\alpha}_2\overline{\beta}_1}{8\omega_0(4\omega_0^2-\omega_1^2)}a^3 + \dfrac{\overline{\alpha}_2\overline{\beta}_1}{4\omega_0\omega_1^2}a^3 - \dfrac{\overline{\alpha}_3\overline{\vartheta}_1}{8\omega_0(4\omega_0^2-\omega_3^2)}a^3 + \dfrac{\overline{\alpha}_3\overline{\vartheta}_1}{4\omega_0\omega_3^2}a^3 \\ -\dfrac{\overline{\alpha}_4\overline{\psi}_1}{8\omega_0(4\omega_0^2-\omega_5^2)}a^3 + \dfrac{\overline{\alpha}_4\overline{\psi}_1}{4\omega_0\omega_5^2}a^3 = -\dfrac{1}{2\omega_0}\widetilde{f}_n \cos(\eta T_2 - \varsigma). \end{cases} \tag{78}$$

Therefore, it can be concluded that

$$\begin{aligned} \eta = & \Big(\frac{3\overline{\alpha}_1}{8\omega_0} + \frac{\overline{\alpha}_2\overline{\beta}_1}{8\omega_0(4\omega_0^2-\omega_1^2)} - \frac{\overline{\alpha}_2\overline{\beta}_1}{4\omega_0\omega_1^2} + \frac{\overline{\alpha}_3\overline{\vartheta}_1}{8\omega_0(4\omega_0^2-\omega_3^2)} - \frac{\overline{\alpha}_3\overline{\vartheta}_1}{4\omega_0\omega_3^2} \\ & + \frac{\overline{\alpha}_4\overline{\psi}_1}{8\omega_0(4\omega_0^2-\omega_5^2)} - \frac{\overline{\alpha}_4\overline{\psi}_1}{4\omega_0\omega_5^2}\Big)a^2 \pm \sqrt{\frac{\widetilde{f}_n^2}{4a^2\omega_0^2} - \xi_{1,n}^2\omega_0^2}. \end{aligned} \tag{79}$$

4 Results and discussion

In this section, the frequency-response and amplitude-response associated with the nonlinear primary resonance of a silicon nanoshell are given corresponding to various interaction between vibration modes. The mechanical properties and surface elastic constants of silicon material are given in Table 1. It is assumed that $L/R = 2$ which results in $m = 1$ and $n = 5$.

Table 1 Material properties of a nanoshell made of silicon[44–45]

Variable	Value
E/GPa	210
v	0.24
$\mu_s/(\mathrm{N\cdot m^{-1}})$	−2.774
$\lambda_s/(\mathrm{N\cdot m^{-1}})$	−4.488
$\tau_s/(\mathrm{N\cdot m^{-1}})$	0.604 8

First, the validity of the present solution methodology is checked. For this purpose, the linear natural frequencies of a single-walled carbon nanotube modeled via the classical shell theory are obtained and compared with those reported by Zeighampour and Tadi Beni[46] using the Navier-type of the exact solution. As tabulated in Table 2, excellent agreement is found which confirms the validity and accuracy of the current study.

Table 2 Comparison of the dimensionless linear frequencies of a single-walled carbon nanotube corresponding to different mode numbers ($h/R = 0.02$, $R = 2.32$ nm, $E = 1.06$ TPa, and $L/R = 5$)

Natural frequency	Ref. [63]	Present study
$m = 1$, $n = 1$	0.196 86	0.197 68
$m = 2$, $n = 2$	0.256 32	0.254 37
$m = 3$, $n = 3$	0.277 30	0.277 12
$m = 4$, $n = 4$	0.301 78	0.302 23
$m = 5$, $n = 5$	0.343 75	0.347 81

The stability analysis is performed for the nonlinear primary resonance of a soft harmonic excited nanoshell including the interaction between all considered vibration modes (the main mode and the first, third, and fifth symmetric modes). In Figs. 2 and 3, the frequency-response and amplitude-response are plotted, respectively, in which the stable and unstable parts of the

responses and the associated bifurcation points are indicated. It is revealed that for very high and very low values of the detuning parameter, the structure is stable. Through increment in the value of the detuning parameter, the deflection of the structure increases until approaching the first saddle-node bifurcation point. After that, the structure becomes unstable as by decreasing the value of the detuning parameter, the shell deflection increases. Thin increment continues up to a peak representing the second saddle-node bifurcation point. Subsequently, the structure becomes stable again in such a way by increasing the detuning parameter, while the deflection of nanoshell reduces.

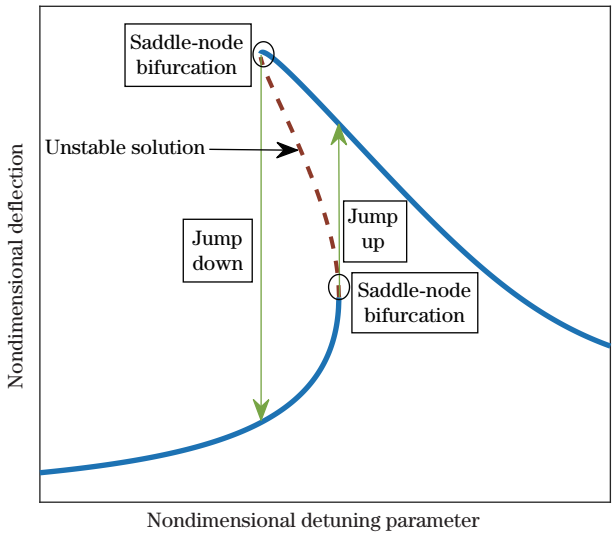

Fig. 2 Stability analysis for the frequency-response associated with the nonlinear primary resonance of a nanoshell incorporating the main mode and 1st, 3rd, and 5th symmetric modes

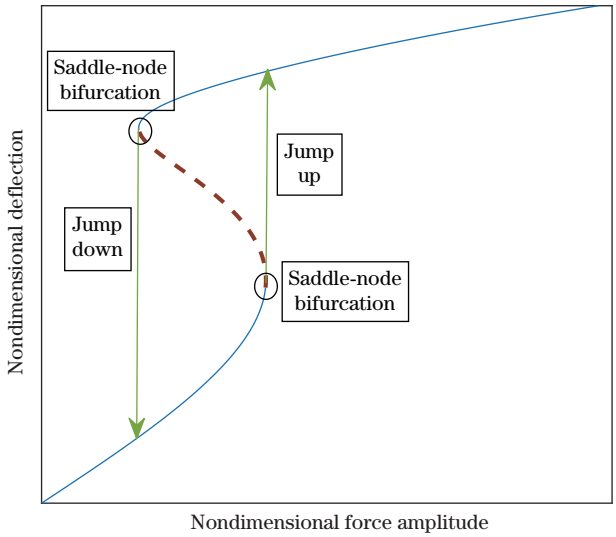

Fig. 3 Stability analysis for the amplitude-response associated with the nonlinear primary resonance of a nanoshell incorporating the main mode and 1st, 3rd, and 5th symmetric modes

Figure 4 represents the influence of different vibration mode interactions on the nonlinear free vibration behavior of a silicon nanoshell in the presence of surface free energy effects. It is seen that by considering only the main vibration mode, the plot curves to the right side representing

a hardening response. However, by adding the interaction between the first symmetric mode and the main mode, the curvature to the right side reduces. After that, the addition of higher symmetric modes including the third and fifth symmetric modes, the frequency-response plot curves to the left side which shows a softening behavior.

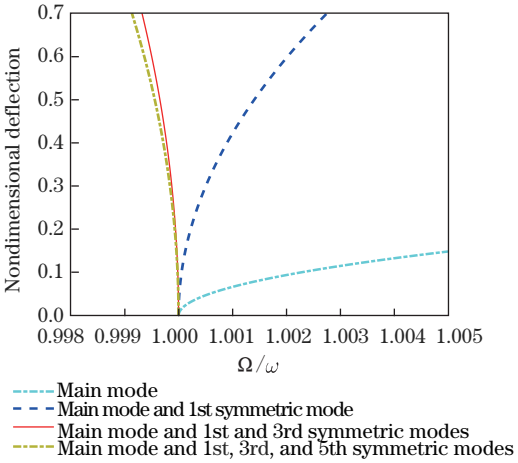

Fig. 4 Influence of the interaction between vibration modes on the frequency-response associated with the nonlinear free vibrations of a nanoshell

In Fig. 5, the influence of various interactions between vibrations mode on the frequency-response and amplitude-response associated with the nonlinear primary resonance of a silicon nanoshell is depicted incorporating surface free energy effects. It is found that by adding the interaction between higher symmetric vibrations modes (the third and fifth ones), the jump phenomenon tends to the left side which indicates a softening behavior. Consequently, for a negative value of the detuning parameter, the amplitude-response including only the interaction between the main mode and the first symmetric mode has no unstable part.

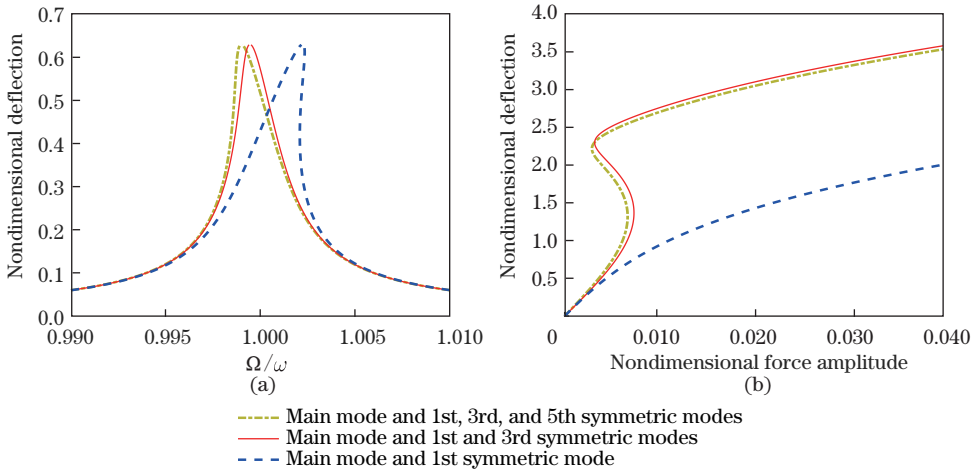

Fig. 5 Influence of the interaction between vibration modes on the nonlinear primary resonance of a nanoshell under harmonic excitation, (a) the frequency-response and (b) the amplitude-response

Figure 6 illustrates the surface free energy effects on the frequency-response and amplitude-response of silicon nanoshells with different shell thicknesses including the interaction between vibration modes. It is observed that by increasing the shell thickness, the surface effects diminish

and the responses tend to the classical counterparts. It is indicated that the surface free energy effects cause to reduce the height of the jump phenomenon. Also, by taking the surface effects into account, the shell deflection as well as the force amplitude associated with both of the bifurcation points enhances.

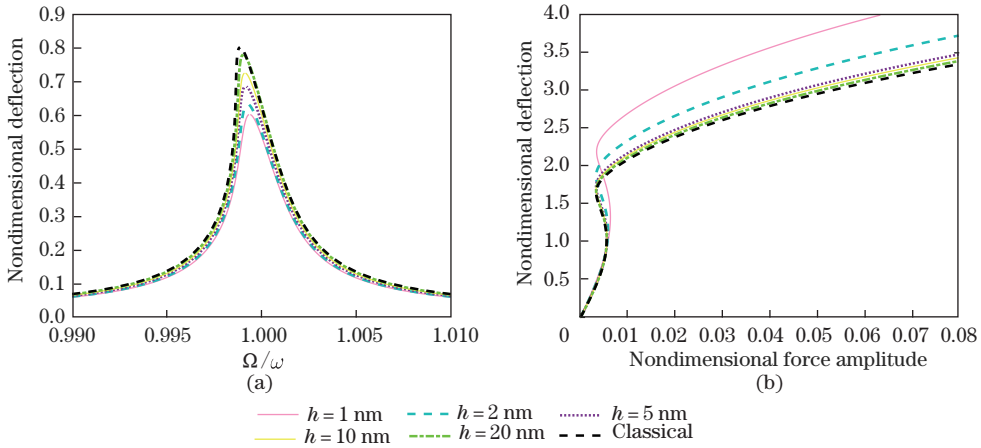

Fig. 6 Classical and non-classical nonlinear primary resonance responses of a nanoshell including the interaction between vibration modes, (a) the frequency-response and (b) the amplitude-response

The influence of surface elastic constants on the frequency-response and amplitude-response associated with the nonlinear primary resonance of a soft harmonic excited nanoshell is shown in Fig. 7 including the interaction between the main vibration mode and the symmetric modes. It can be seen that a positive value of the surface elastic constants leads to a decrease in the height of the jump phenomenon as well as the shell deflection associated with both of the bifurcation points, while a negative one causes to increase them.

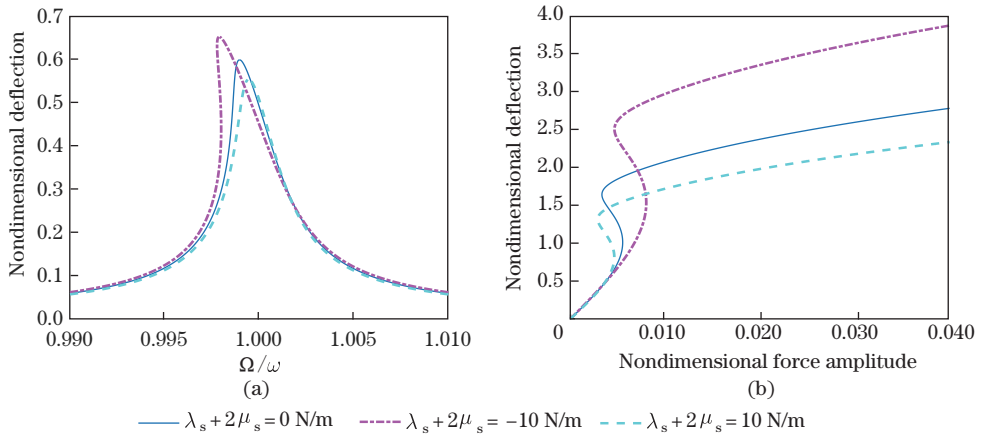

Fig. 7 Influence of the surface elastic constants on the nonlinear primary resonance of a nanoshell including the interaction between vibration modes, (a) the frequency-response and (b) the amplitude-response

In Fig. 8, the influence of the surface residual stress on the frequency-response and amplitude-response associated with the nonlinear primary resonance of a soft harmonic excited nanoshell is displayed including the interaction between the main vibration mode and the symmetric modes. It is found that a positive value of the surface residual stress makes a reduction in the height of the jump phenomenon as well as the force amplitude associated with both of the bifurcation points, while a negative one leads to an increase in them.

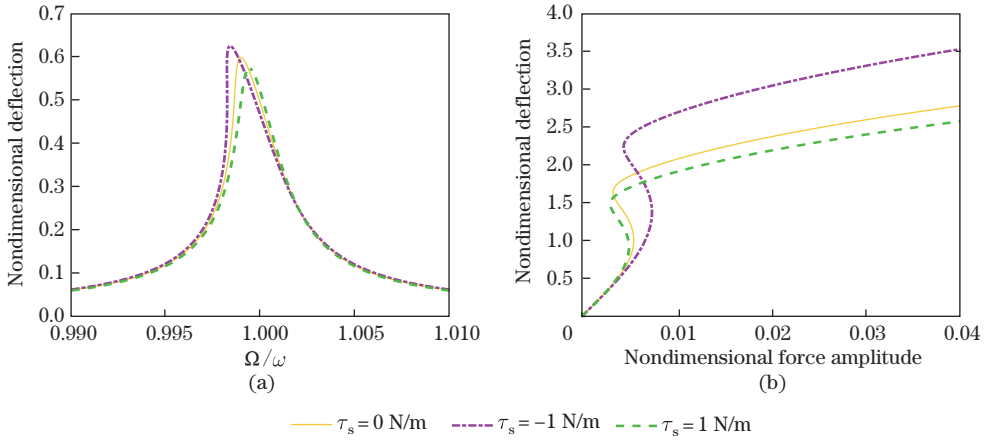

Fig. 8 Influence of the surface residual stress on the nonlinear primary resonance of a nanoshell including the interaction between vibration modes, (a) the frequency-response and (b) the amplitude-response

Figures 9 and 10 demonstrate the influence of the interaction between vibration modes on the nonlinear primary resonance characteristics of a soft harmonic excited nanoshell corresponding to various values of surface elastic constants and surface residual stress, respectively. It is revealed that for both of the positive and negative values of the surface parameters, by adding the interaction between higher symmetric vibration modes with the main mode, the hardening behavior changes to the softening one. As a result, for a negative value of the detuning parameter, the amplitude-response plot including only the interaction between the first symmetric mode and the main mode has no unstable part. However, by taking the third and fifth symmetric modes into consideration, the unstable part with the two saddle-node bifurcation points can be observed.

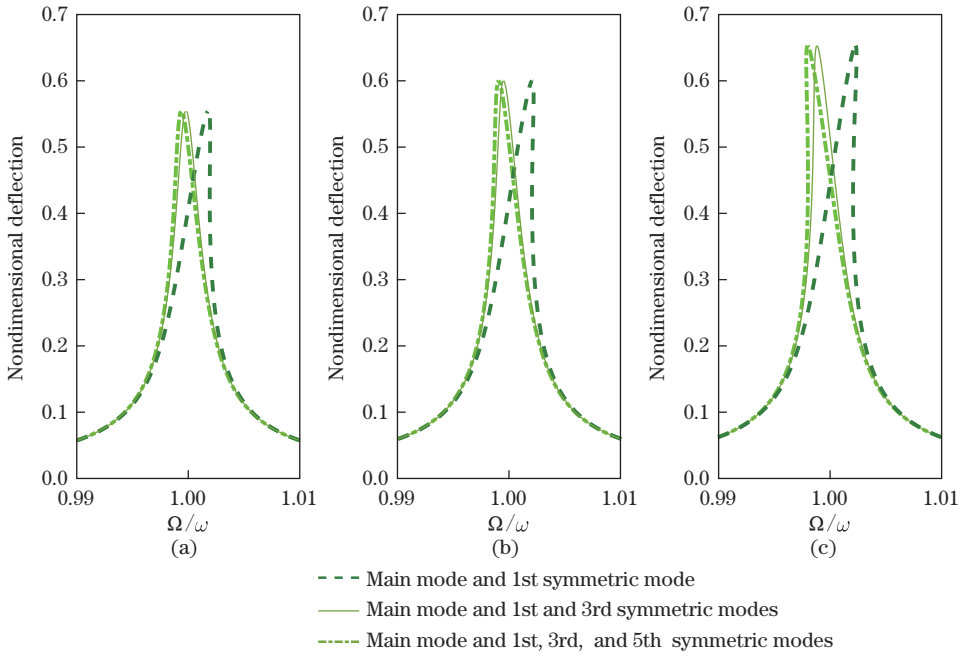

Fig. 9 Influence of the interaction between vibration modes on the nonlinear primary resonance response corresponding to different surface elastic constants, (a) $\lambda_s + 2\mu_s = -10$ N/m, (b) $\lambda_s + 2\mu_s = 0$ N/m, and (c) $\lambda_s + 2\mu_s = 10$ N/m

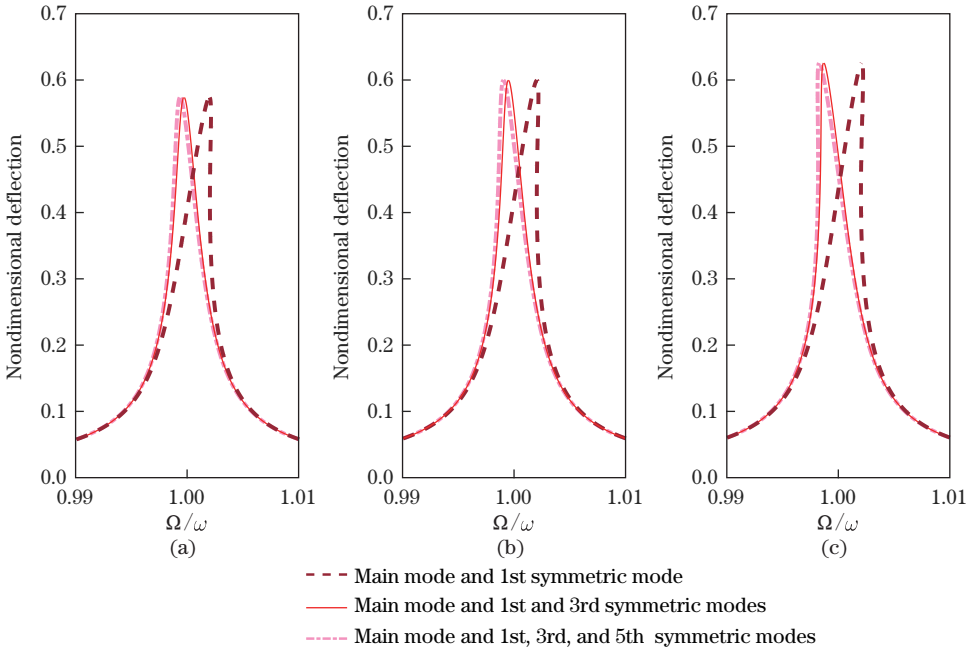

Fig. 10 Influence of the interaction between vibration modes on the nonlinear primary resonance response corresponding to different surface residual stresses, (a) $\tau_s = -1$ N/m, (b) $\tau_s = 0$ N/m, and (c) $\tau_s = -1$ N/m

5 Conclusions

In this investigation, for the first time, the nonlinear primary resonance response of soft harmonic excited nanoshells including the surface free energy effects and interaction between vibration modes was studied. To the end, the Gurtin-Murdoch theory of elasticity was implemented into the classical shell theory to develop a non-classical shell model with the capability to capture the surface effects. Afterward, with the aid of the multi-time-scale method, the size-dependent nonlinear governing differential equations of motion were solved analytically corresponding to various interactions between the main mode and symmetric vibration modes.

It was displayed that by adding the interaction between higher symmetric vibrations modes (the third and fifth ones), the jump phenomenon tends to shift from the hardening response to the softening one. Consequently, for a negative value of the detuning parameter, the amplitude-response including only the interaction between the main mode and the first symmetric mode has no unstable part. Furthermore, it was found that by increasing the shell thickness, the surface effects diminish and the responses tend to the classical counterparts. It was seen that the surface free energy effects cause to reduce the height of the jump phenomenon. Also, by taking the surface effects into account, the shell deflection as well as the force amplitude associated with both of the bifurcation points enhances. Additionally, it was observed that a positive value of the surface residual stress makes a reduction in the height of the jump phenomenon as well as the force amplitude associated with both of the bifurcation points, while a negative one leads to increasing them.

References

[1] TOGUN, N. and BAGDATLI, S. M. Size dependent nonlinear vibration of the tensioned nanobeam based on the modified couple stress theory. *Composites Part B: Engineering*, **97**, 255–262 (2016)

[2] BORNASSI, S. and HADDADPOUR, H. Nonlocal vibration and pull-in instability analysis of electrostatic carbon-nanotube based NEMS devices. *Sensors and Actuators A*: *Physical*, **266**, 185–196 (2017)

[3] GUO, J., CHEN, J., and PAN, E. Free vibration of three-dimensional anisotropic layered composite nanoplates based on modified couple-stress theory. *Physica E*, **87**, 98–106 (2017)

[4] LI, C., LIU, J. J., CHENG, M., and FAN, X. L. Modeling of nonlinear vibration of graphene sheets using a meshfree method based on nonlocal elasticity theory. *Composites Part B*: *Engineering*, **116**, 153–169 (2017)

[5] ZHANG, L. W., ZHANG, Y., and LIEW, K. M. Modeling of nonlinear vibration of graphene sheets using a meshfree method based on nonlocal elasticity theory. *Applied Mathematical Modelling*, **49**, 691–704 (2017)

[6] LU, L., GUO, X., and ZHAO, J. Size-dependent vibration analysis of nanobeams based on the nonlocal strain gradient theory. *International Journal of Engineering Science*, **116**, 12–24 (2017)

[7] LIU, J. C., ZHANG, Y. Q., and FAN, L. F. Nonlocal vibration and biaxial buckling of double-viscoelastic-FGM-nanoplate system with viscoelastic Pasternak medium in between. *Physics Letters A*, **381**, 1228–1235 (2017)

[8] ZHANG, H., WANG, C. M., and CHALLAMEL, N. Novel differential quadrature element method for vibration analysis of hybrid nonlocal Euler-Bernoulli beams. *Composite Structures*, **165**, 148–159 (2017)

[9] YANG, Z. and HE, D. Vibration and buckling of orthotropic functionally graded micro-plates on the basis of a re-modified couple stress theory. *Results in Physics*, **7**, 3778–3787 (2017)

[10] FANG, J., GU, J., and WANG, H. Size-dependent three-dimensional free vibration of rotating functionally graded microbeams based on a modified couple stress theory. *International Journal of Mechanical Sciences*, **136**, 188–199 (2017)

[11] APUZZO, A., BARRETTA, R., FAGHIDIAN, S. A., LUCIANO, R., and MORATTI DE SCIARRA, F. Free vibrations of elastic beams by modified nonlocal strain gradient theory. *International Journal of Engineering Science*, **133**, 99–108 (2018)

[12] KIANI, K. and PAKDAMAN, H. Nonlocal vibrations and potential instability of monolayers from double-walled carbon nanotubes subjected to temperature gradients. *International Journal of Mechanical Sciences*, **144**, 576–599 (2018)

[13] WANG, J., SHEN, H., ZHANG, B., LIU, J., and ZHANG, Y. Complex modal analysis of transverse free vibrations for axially moving nanobeams based on the nonlocal strain gradient theory. *Physica E*, **101**, 85–93 (2018)

[14] THANH, C. L., PHUNG-VAN, P., THAI, C. H., NGUYEN-XUAN, N., and ABDEL-WAHAB, M. Isogeometric analysis of functionally graded carbon nanotube reinforced composite nanoplates using modified couple stress theory. *Composite Structures*, **184**, 633–649 (2018)

[15] SAHMANI, S., AGHDAM, M. M., and RABCZUK, T. Nonlocal strain gradient plate model for nonlinear large-amplitude vibrations of functionally graded porous micro/nano-plates reinforced with GPLs. *Composite Structures*, **198**, 51–62 (2018)

[16] SAHMANI, S., AGHDAM, M. M., and RABCZUK, T. A unified nonlocal strain gradient plate model for nonlinear axial instability of functionally graded porous micro/nano-plates reinforced with graphene platelets. *Materials Research Express*, **5**, 045048 (2018)

[17] SAHMANI, S., AGHDAM, M. M., and RABCZUK, T. Nonlinear bending of functionally graded porous micro/nano-beams reinforced with graphene platelets based upon nonlocal strain gradient theory. *Composite Structures*, **186**, 68–78 (2018)

[18] WANG, X. Novel differential quadrature element method for vibration analysis of hybrid nonlocal Euler-Bernoulli beams. *Applied Mathematics Letters*, **77**, 94–100 (2018)

[19] SHEN, J. P., WANG, P. Y., LI, C., and WANG, Y. Y. New observations on transverse dynamics of microtubules based on nonlocal strain gradient theory. *Composite Structures*, **225**, 111036 (2019)

[20] TANG, H., LI, L., HU, Y., MENG, W., and DUAN, K. Vibration of nonlocal strain gradient beams incorporating Poisson's ratio and thickness effects. *Thin-Walled Structures*, **137**, 377–391 (2019)

[21] JALAEI, M. H., GHORBANPOUR-ARANI, A., and NGUYEN-XUAN, H. Investigation of thermal and magnetic field effects on the dynamic instability of FG Timoshenko nanobeam employing nonlocal strain gradient theory. *International Journal of Mechanical Sciences*, **161**, 105043 (2019)

[22] SAHMANI, S. and SAFAEI, B. Nonlinear free vibrations of bi-directional functionally graded micro/nano-beams including nonlocal stress and microstructural strain gradient size effects. *Thin-Walled Structures*, **140**, 342–356 (2019)

[23] SAHMANI, S. and SAFAEI, B. Nonlocal strain gradient nonlinear resonance of bi-directional functionally graded composite micro/nano-beams under periodic soft excitation. *Thin-Walled Structures*, **143**, 106226 (2019)

[24] JALAEI, M. H. and CIVALEK, O. A nonlocal strain gradient refined plate theory for dynamic instability of embedded graphene sheet including thermal effects. *Composite Structures*, **220**, 209–220 (2019)

[25] ZHANG, B., SHEN, H., LIU, J., WANG, Y., and ZHANG, Y. Deep postbuckling and nonlinear bending behaviors of nanobeams with nonlocal and strain gradient effects. *Applied Mathematics and Mechanics* (*English Edition*), **40**(4), 515–548 (2019) https://doi.org/10.1007/s10483-019-2482-9

[26] SAHMANI, S., FATTAHI, A. M., and AHMED, N. A. Analytical mathematical solution for vibrational response of postbuckled laminated FG-GPLRC nonlocal strain gradient micro-/nanobeams. *Engineering with Computers*, **35**, 1173–1189 (2019)

[27] WANG, Y., LIU, Y., and ZU, J. W. Nonlinear free vibration of piezoelectric cylindrical nanoshells. *Applied Mathematics and Mechanics* (*English Edition*), **40**(5), 601–620 (2019) https://doi.org/10.1007/s10483-019-2476-6

[28] GURTIN, M. E. and MURDOCH, A. I. A continuum theory of elastic material surface. *Archive for Rational Mechanics and Analysis*, **57**, 291–323 (1975)

[29] GURTIN, M. E. and MURDOCH, A. I. Surface stress in solids. *International Journal of Solids and Structures*, **14**, 431–440 (1978)

[30] WANG, G. F. and FENG, X. Q. Effects of surface elasticity and residual surface tension on the natural frequency of microbeams. *Applied Physics Letters*, **90**, 231904 (2007)

[31] LUO, J. and XIAO, Z. M. Analysis of a screw dislocation interacting with an elliptical nano inhomogeneity. *International Journal of Engineering Science*, **47**, 883–893 (2009)

[32] ZHAO, X. J. and RAJAPAKSE, R. K. N. D. Analytical solutions for a surface loaded isotropic elastic layer with surface energy effects. *International Journal of Engineering Science*, **47**, 1433–1444 (2009)

[33] WANG, Z. Q., ZHAO, Y. P., and HUANG, Z. P. The effects of surface tension on the elastic properties of nano structures. *International Journal of Engineering Science*, **48**, 140–150 (2010)

[34] CHIU, M. S. and CHEN, T. Bending and resonance behavior of nanowires based on Timoshenko beam theory with high-order surface stress effects. *Physica E*, **54**, 149–156 (2013)

[35] SHAAT, M., MAHMOUD, F. F., GAO, X. L., and FAHEEM, A. F. Size-dependent bending analysis of Kirchhoff nano-plates based on a modified couple-stress theory including surface effects. *International Journal of Mechanical Sciences*, **79**, 31–37 (2014)

[36] SAHMANI, S., BAHRAMI, M., AGHDAM, M. M., and ANSARI, R. Surface effects on the nonlinear forced vibration response of third-order shear deformable nanobeams. *Composite Structures*, **118**, 149–158 (2014)

[37] SAHMANI, S. and AGHDAM, M. M. Imperfection sensitivity of the size-dependent postbuckling response of pressurized FGM nanoshells in thermal environments. *Archives of Civil and Mechanical Engineering*, **17**, 623–638 (2017)

[38] LU, L., GUO, X., and ZHAO, J. On the mechanics of Kirchhoff and Mindlin plates incorporating surface energy. *International Journal of Engineering Science*, **124**, 24–40 (2018)

[39] SUN, J., WANG, Z., ZHOU, Z., XU, X., and LIM, C. W. Surface effects on the buckling behaviors of piezoelectric cylindrical nanoshells using nonlocal continuum model. *Applied Mathematical Modelling*, **59**, 341–356 (2018)

[40] LU, L., GUO, X., and ZHAO, J. A unified size-dependent plate model based on nonlocal strain gradient theory including surface effects. *Applied Mathematical Modelling*, **68**, 583–602 (2019)

[41] SARAFRAZ, A., SAHMANI, S., and AGHDAM, M. M. Nonlinear secondary resonance of nanobeams under subharmonic and superharmonic excitations including surface free energy effects. *Applied Mathematical Modelling*, **66**, 195–226 (2019)

[42] AMABILI, M., PELLICANO, F., and PAIDOUSSISI M. Non-linear dynamics and stability of circular cylindrical shells containing flowing fluid, part II: large-amplitude vibrations without flow. *Journal of Sound and Vibration*, **228**, 1103–1124 (1999)

[43] AMABILI, M. and PAIDOUSSIS, M. P. Review of studies on geometrically nonlinear vibrations and dynamics of circular cylindrical shells and panels, with and without fluid-structure interaction. *Applied Mechanics Reviews*, **56**, 349–381 (2003)

[44] MILLER, R. E. and SHENOY, V. B. Size-dependent elastic properties of nanosized structural elements. *Nanotechnology*, **11**, 139–147 (2000)

[45] ZHU, R., PAN, E., CHUNG, P. W., CAI, X., LIEW, K. M., and BULDUM, A. Atomistic calculation of elastic moduli in strained silicon. *Semiconductor Science and Technology*, **21**, 906–911 (2006)

[46] ZEIGHAMPOUR, H. and TADI BENI, Y. Cylindrical thin-shell model based on modified strain gradient theory. *International Journal of Engineering Science*, **78**, 27–47 (2014)

Appendix A

The parameters of $c_i(t)$ with $i = 1, 2, \cdots, 10$ are presented as follows:

$$\begin{cases} c_1(t) = \dfrac{\eta\pi^2 A_{1,n}}{\Big(\xi^2\eta^2\pi^4 + \Big(\dfrac{\eta}{\xi}\Big)^2 n^4\Big)\overline{\Gamma}_1 + \eta^2\pi^2 n^2(\overline{\Gamma}_2 - 2\overline{\Gamma}_5)}, \\ c_2(t) = \dfrac{A_{1,0}}{\xi^2\eta\pi^2\overline{\Gamma}_1}, \\ c_3(t) = \dfrac{A_{3,0}}{9\xi^2\eta\pi^2\overline{\Gamma}_1}, \\ c_4(t) = \dfrac{A_{5,0}}{25\xi^2\eta\pi^2\overline{\Gamma}_1}, \\ c_5(t) = \dfrac{n^2 A_{1,n}^2}{32\xi^2\pi^2\overline{\Gamma}_1}, \\ c_6(t) = \dfrac{\xi^2\pi^2 A_{1,n}A_{1,0}}{2n^2\overline{\Gamma}_1}, \\ c_7(t) = \dfrac{n^2\eta^2\pi^2 A_{1,n}(A_{1,0} - 9A_{3,0})}{2\Big(16\xi^2\eta^2\pi^4 + \Big(\dfrac{\eta}{\xi}\Big)^2 n^4\Big)\overline{\Gamma}_1 + 8\eta^2\pi^2 n^2(\overline{\Gamma}_2 - 2\overline{\Gamma}_5)}, \\ c_8(t) = \dfrac{n^2\eta^2\pi^2 A_{1,n}(9A_{3,0} - 25A_{5,0})}{2\Big(256\xi^2\eta^2\pi^4 + \Big(\dfrac{\eta}{\xi}\Big)^2 n^4\Big)\overline{\Gamma}_1 + 32\eta^2\pi^2 n^2(\overline{\Gamma}_2 - 2\overline{\Gamma}_5)}, \\ c_9(t) = \dfrac{25n^2\eta^2\pi^2 A_{1,n}A_{5,0}}{2\Big(1\,296\xi^2\eta^2\pi^4 + \Big(\dfrac{\eta}{\xi}\Big)^2 n^4\Big)\overline{\Gamma}_1 + 36\eta^2\pi^2 n^2(\overline{\Gamma}_2 - 2\overline{\Gamma}_5)}, \\ c_{10}(t) = -\dfrac{\xi^2\pi^2 A_{1,n}^2}{32n^2\overline{\Gamma}_1}. \end{cases}$$

Appendix B

The following sets of equations corresponding to different orders of ε of the main and first symmetric vibration modes are obtained:

$$\varepsilon^0 \rightarrow \begin{cases} D_0^2 q_{10} + \omega_0^2 q_{10} = 0, \\ D_0^2 q_{20} + \omega_1^2 q_{20} = 0, \end{cases}$$

$$
\varepsilon^1 \rightarrow \begin{cases} D_0^2 q_{11} + \omega_0^2 q_{11} = -2D_0 D_1 q_{10} - \overline{\alpha}_2 q_{10} q_{20}, \\ D_0^2 q_{21} + \omega_1^2 q_{21} = -2D_0 D_1 q_{20} - \overline{\beta}_2 q_{10}^2, \end{cases}
$$

$$
\varepsilon^2 \rightarrow \begin{cases} D_0^2 q_{12} + \omega_0^2 q_{12} = -2D_0 D_1 q_{11} - D_1^2 q_{10} - 2D_0 D_1 q_{10} - 2\xi_{1,n}\omega_0 D_0 q_{10} - \overline{\alpha}_1 q_{10}^3 \\ \qquad\qquad -\overline{\alpha}_2 q_{10} q_{21} - \overline{\alpha}_2 q_{20} q_{11} - \overline{\alpha}_5 q_{10} q_{20}^2 + \dfrac{1}{2}\widetilde{f}_n \mathrm{e}^{\mathrm{i}(\omega_0 T_0 + \eta T_2)}, \\ D_0^2 q_{22} + \omega_1^2 q_{22} = -2D_0 D_1 q_{21} - D_1^2 q_{20} - 2D_0 D_1 q_{20} - 2\xi_{1,0}\omega_1 D_0 q_{20} - 2\overline{\beta}_1 q_{10} q_{11} \\ \qquad\qquad -\overline{\beta}_2 q_{20} q_{10}^2. \end{cases}
$$

The following sets of equations corresponding to different orders of ε of the main, first, and third symmetric vibration modes are obtained:

$$
\varepsilon^0 \rightarrow \begin{cases} D_0^2 q_{10} + \omega_0^2 q_{10} = 0, \\ D_0^2 q_{20} + \omega_1^2 q_{20} = 0, \\ D_0^2 q_{30} + \omega_3^2 q_{30} = 0, \end{cases}
$$

$$
\varepsilon^1 \rightarrow \begin{cases} D_0^2 q_{11} + \omega_0^2 q_{11} = -2D_0 D_1 q_{10} - \overline{\alpha}_2 q_{10} q_{20} - \overline{\alpha}_3 q_{10} q_{30}, \\ D_0^2 q_{21} + \omega_1^2 q_{21} = -2D_0 D_1 q_{20} - \overline{\beta}_1 q_{10}^2, \\ D_0^2 q_{31} + \omega_3^2 q_{31} = -2D_0 D_1 q_{30} - \overline{\vartheta}_1 q_{10}^2, \end{cases}
$$

$$
\varepsilon^2 \rightarrow \begin{cases} D_0^2 q_{12} + \omega_0^2 q_{12} = -2D_0 D_1 q_{11} - D_1^2 q_{10} - 2D_0 D_1 q_{10} - 2\xi_{1,n}\omega_0 D_0 q_{10} - \overline{\alpha}_1 q_{10}^3 \\ \qquad\qquad -\overline{\alpha}_2 q_{10} q_{21} - \overline{\alpha}_2 q_{20} q_{11} - \overline{\alpha}_3 q_{30} q_{11} - \overline{\alpha}_5 q_{10} q_{20}^2 \\ \qquad\qquad -\overline{\alpha}_6 q_{10} q_{30}^2 - \overline{\alpha}_8 q_{10} q_{20} q_{30} + \dfrac{1}{2}\widetilde{f}_n \mathrm{e}^{\mathrm{i}(\omega_0 T_0 + \eta T_2)}, \\ D_0^2 q_{22} + \omega_1^2 q_{22} = -2D_0 D_1 q_{21} - D_1^2 q_{20} - 2D_0 D_1 q_{20} - 2\xi_{1,0}\omega_1 D_0 q_{20} - 2\overline{\beta}_1 q_{10} q_{11} \\ \qquad\qquad -\overline{\beta}_2 q_{20} q_{10}^2 - \overline{\beta}_3 q_{30} q_{10}^2, \\ D_0^2 q_{32} + \omega_3^2 q_{32} = -2D_0 D_1 q_{31} - D_1^2 q_{30} - 2D_0 D_1 q_{30} - 2\xi_{3,0}\omega_3 D_0 q_{30} - 2\overline{\vartheta}_1 q_{10} q_{11} \\ \qquad\qquad -\overline{\vartheta}_2 q_{20} q_{10}^2 - \overline{\vartheta}_3 q_{30} q_{10}^2. \end{cases}
$$

The following sets of equations corresponding to different orders of ε of the main, first, third, and fifth symmetric vibration modes are obtained:

$$
\varepsilon^0 \rightarrow \begin{cases} D_0^2 q_{10} + \omega_0^2 q_{10} = 0, \\ D_0^2 q_{20} + \omega_1^2 q_{20} = 0, \\ D_0^2 q_{30} + \omega_3^2 q_{30} = 0, \\ D_0^2 q_{40} + \omega_5^2 q_{40} = 0, \end{cases}
$$

$$
\varepsilon^1 \rightarrow \begin{cases} D_0^2 q_{11} + \omega_0^2 q_{11} = -2D_0 D_1 q_{10} - \overline{\alpha}_2 q_{10} q_{20} - \overline{\alpha}_3 q_{10} q_{30} - \overline{\alpha}_4 q_{10} q_{40}, \\ D_0^2 q_{21} + \omega_1^2 q_{21} = -2D_0 D_1 q_{20} - \overline{\beta}_1 q_{10}^2, \\ D_0^2 q_{31} + \omega_3^2 q_{31} = -2D_0 D_1 q_{30} - \overline{\vartheta}_1 q_{10}^2, \\ D_0^2 q_{41} + \omega_5^2 q_{41} = -2D_0 D_1 q_{40} - \overline{\psi}_1 q_{10}^2, \end{cases}
$$

$$
\varepsilon^2 \rightarrow \begin{cases} D_0^2 q_{12} + \omega_0^2 q_{12} = -2D_0 D_1 q_{11} - D_1^2 q_{10} - 2D_0 D_1 q_{10} - 2\xi_{1,n}\omega_0 D_0 q_{10} - \overline{\alpha}_1 q_{10}^3 \\ \qquad\qquad -\overline{\alpha}_2 q_{10} q_{21} - \overline{\alpha}_2 q_{20} q_{11} - \overline{\alpha}_3 q_{10} q_{31} - \overline{\alpha}_3 q_{30} q_{11} - \overline{\alpha}_4 q_{10} q_{41} \\ \qquad\qquad -\overline{\alpha}_4 q_{40} q_{11} - \overline{\alpha}_5 q_{10} q_{20}^2 - \overline{\alpha}_6 q_{10} q_{30}^2 - \overline{\alpha}_7 q_{10} q_{40}^2 \\ \qquad\qquad -\overline{\alpha}_8 q_{10} q_{20} q_{30} - \overline{\alpha}_9 q_{10} q_{30} q_{40} + \dfrac{1}{2}\widetilde{f}_n \mathrm{e}^{\mathrm{i}(\omega_0 T_0 + \eta T_2)}, \\ D_0^2 q_{22} + \omega_1^2 q_{22} = -2D_0 D_1 q_{21} - D_1^2 q_{20} - 2D_0 D_1 q_{20} - 2\xi_{1,0}\omega_1 D_0 q_{20} - 2\overline{\beta}_1 q_{10} q_{11} \\ \qquad\qquad -\overline{\beta}_2 q_{20} q_{10}^2 - \overline{\beta}_3 q_{30} q_{10}^2, \\ D_0^2 q_{32} + \omega_3^2 q_{32} = -2D_0 D_1 q_{31} - D_1^2 q_{30} - 2D_0 D_1 q_{30} - 2\xi_{3,0}\omega_3 D_0 q_{30} - 2\overline{\vartheta}_1 q_{10} q_{11} \\ \qquad\qquad -\overline{\vartheta}_2 q_{20} q_{10}^2 - \overline{\vartheta}_3 q_{30} q_{10}^2 - \overline{\vartheta}_4 q_{40} q_{10}^2, \\ D_0^2 q_{42} + \omega_5^2 q_{42} = -2D_0 D_1 q_{41} - D_1^2 q_{40} - 2D_0 D_1 q_{40} - 2\xi_{5,0}\omega_5 D_0 q_{40} - 2\overline{\psi}_1 q_{10} q_{11} \\ \qquad\qquad -\overline{\psi}_2 q_{30} q_{10}^2 - \overline{\psi}_3 q_{40} q_{10}^2. \end{cases}
$$